survival signaling in murine hematopoietic progenitors. Mol. Cell. Biol. 21:854–864.

45. Silva, M., A. Benito, C. Sanz, F. Prosper, D. Ekhterae, G. Nunez, and J. L. Fernandez-Luna. 1999. Erythropoietin can induce the expression of bcl-x(L) through Stat5 in erythropoietin-dependent progenitor cell lines. J. Biol. Chem. 274:22165–22169.

46. Socolovsky, M., A. E. Fallon, S. Wang, C. Brugnara, and H. F. Lodish. 1999. Fetal anemia and apoptosis of red cell progenitors in Stat5a$^{-/-}$5b$^{-/-}$ mice: a direct role for Stat5 in Bcl-X(L) induction. Cell 98:181–191.

47. Veis, D. J., C. M. Sorenson, J. R. Shutter, and S. J. Korsmeyer. 1993. Bcl-2-deficient mice demonstrate fulminant lymphoid apoptosis, polycystic kidneys, and hypopigmented hair. Cell 75:229–240.

48. Weston, C. R., K. Balmanno, C. Chalmers, K. Hadfield, S. A. Molton, R. Ley, E. F. Wagner, and S. J. Cook. 2003. Activation of ERK1/2 by deltaRaf-1:ER* represses Bim expression independently of the JNK or PI3K pathways. Oncogene 22:1281–1293.

49. Whitfield, J., S. J. Neame, L. Paquet, O. Bernard, and J. Ham. 2001. Dominant-negative c-Jun promotes neuronal survival by reducing BIM expression and inhibiting mitochondrial cytochrome c release. Neuron 29:629–643.

50. Yamaguchi, T., T. Okada, T. Takeuchi, T. Tonda, M. Ohtaki, S. Shinoda, T. Masuzawa, K. Ozawa, and T. Inaba. 2003. Enhancement of thymidine kinase-mediated killing of malignant glioma by BimS, a BH3-only cell death activator. Gene Ther. 10:375–385.

SPOTLIGHT CORRESPONDENCE

Interstitial pneumonia induced by imatinib mesylate: pathologic study demonstrates alveolar destruction and fibrosis with eosinophilic infiltration

TO THE EDITOR

Imatinib mesylate (Gleevec, Glivec, formerly, STI571) is an inhibitor of the BCR-ABL tyrosine kinase that is central to the pathogenesis of chronic myelogenous leukemia (CML). A recent large-scale prospective randomized trial, comparing imatinib vs interferon plus cytarabine for chronic phase CML, demonstrated the impressive therapeutic superiority of imatinib.[1] The current therapeutic strategy for CML was reviewed by Hehlmann.[2] Although imatinib is a well-tolerated drug, various adverse events such as superficial edema, nausea, muscle cramps, and skin rash were reported. These events were grades 1–2 in most cases, and medical treatment appears to be feasible.[3] With respect to the respiratory complications, dyspnea and cough have been reported to occur in 7–10 and 10–14% of patients receiving imatinib, respectively,[1,3] although they were ascribed to pulmonary edema. Their causes have not been clearly described. We report a case of an imatinib-induced interstitial pneumonia and its pathologic findings obtained by transbronchial lung biopsy (TBLB) in a patient with CML.

The patient was a 64-year-old man who was first given a diagnosis of CML in June 2001. Thereafter, he received 1000 mg of hydroxycarbamide daily, which resulted in a complete hematological response. After 18 months, his white blood cell (WBC) count increased even though he was still receiving hydroxycarbamide. No hepatosplenomegaly was noted. The bone marrow findings showed a hypercellular marrow with 1.6% blasts, and interphase-FISH analysis revealed the BCR-ABL fusion gene in 89.8% of the bone marrow nucleated cells. Imatinib (400 mg/day) was started in January 2003, resulting in a complete hematological response. However, on the 78th day after initiation of imatinib, he started to suffer dyspnea (Hugh-Jones grade II). At that time, an interphase-FISH analysis revealed the BCR-ABL fusion gene to be present in 92.5% of peripheral neutrophils. Chest X-ray showed bilateral ground-glass opacities in the lower lung fields. Computed tomography (CT) revealed reticular and ground-glass opacities in the subpleural area (Figure 1). Arterial blood measurements showed a pH of 7.418, arterial oxygen pressure of 95.6 mmHg, and carbon dioxide pressure of 43.3 mmHg in room air. No other symptoms, including skin rash and edema, were noted. He did not take other medicines at that time. Laboratory studies revealed that the WBC count was 3.9×10^6/l with 12.7% eosinophils, hemoglobin was 11.2 g/dl, and platelet count was 1.4×10^8/l. The erythrocyte sedimentation rate was 33 mm/h, C-reactive protein was 1.4 mg/l, LDH was 438 U/l (normal range: 224 454 U/l), and KL-6, which indicates an activity of interstitial

pneumonia, was 1 360 U/ml (normal limit: less than 500 U/ml), respectively. Other biochemical data were all within normal ranges. Although a drug lymphocyte-stimulating test (DLST) for imatinib mesylate was negative, imatinib-induced interstitial pneumonia was suspected, because no other cause was evident. Imatinib was discontinued after a total dose of 31 200 mg (400 mg × 78 days). A TBLB revealed the destruction of alveolar septi and mixed intra-alveolar and interstitial fibrosis along with eosinophilic infiltration (Figure 2). Bronchoalveolar lavage fluid could not able to be collected at that time. After cessation of imatinib, the dyspnea improved within 10 days even without steroid therapy. Chest X-ray and CT on the 18th day after cessation of imatinib showed almost complete resolution of interstitial shadows. Since the WBC count re-elevated to 30×10^6/l after discontinuation of imatinib, we began to give hydroxycarbamide, increasing the dosage to 1500 mg/day in May 2003. This resulted in a reduction of the WBC count.

Imatinib mesylate now has been estimated to be used in about 3200 cases in Japan. According to a recent postmarketing surveillance by Novartis Japan, 24 cases of interstitial pneumonia, apparently related to imatinib, have been registered (20 cases of CML, one of hypereosinophilic syndrome, and three cases of gastrointestinal stromal tumor) (Novartis Pharma KK, data on file). Only two of 24 cases had a past history of lung disease; one was interstitial pneumonia and the other was chronic bronchitis. The appearance of interstitial pneumonia ranged from 10 to 337 days (median 42 days) after initiation of imatinib administration. Among these cases, three received 600 mg/day of imatinib, 13 cases received 400 mg/day, and eight cases less than 300 mg/day. In 20 CML patients showing interstitial pneumonia, 35% were in the accelerated/blastic crisis phase and 65% in the chronic phase. In the 14 cases reporting complete blood cell count and WBC differentiation, eight patients (57%) showed eosinophilia, although they had achieved complete hematological response by imatinib at that time. Steroid therapy was carried out in all these cases, and 19 cases recovered; one case did not improve, and one patient died.

The mechanism of drug-induced pneumonia is unclear in the vast majority of cases; however, it is considered to consist of either idiosyncratic (= noncytotoxic type) or cytotoxic type. The latter is dose dependent with pathologic features of interstitial edema, lymphocytic infiltration, destruction of alveolar epithelium etcetera, for example, busulfan lung or bleomycin lung. In contrast, the noncytotoxic type resembles hypersensitivity pneumonia, bronchiolitis obliterans, or eosinophilic pneumonia. We found eosinophilic infitration in the current case; however, we cannot completely rule out the possibility that the underlying disease (CML) may have modified the pathologic features. In the Novartis report, none of the seven cases of imatinib-induced interstitial pneumonia examined were DLST positive. In our case, the pathologic findings of TBLB showing prominent infiltration of eosinophils suggested an immunoallergic mechanism. There is one report showing a case of hypersensitivity pneumonitis related to imatinib, which may also support the immunoallergic background, but that study

Correspondence: T Yokoyama, First Department of Internal Medicine, Tokyo Medical University, 6-7-1 Nishishinjuku, Shinjuku-ku, Tokyo 160-0023, Japan; Fax: +81 3 5381 6651; E-mail: yokoyama@tokyo-med.ac.jp
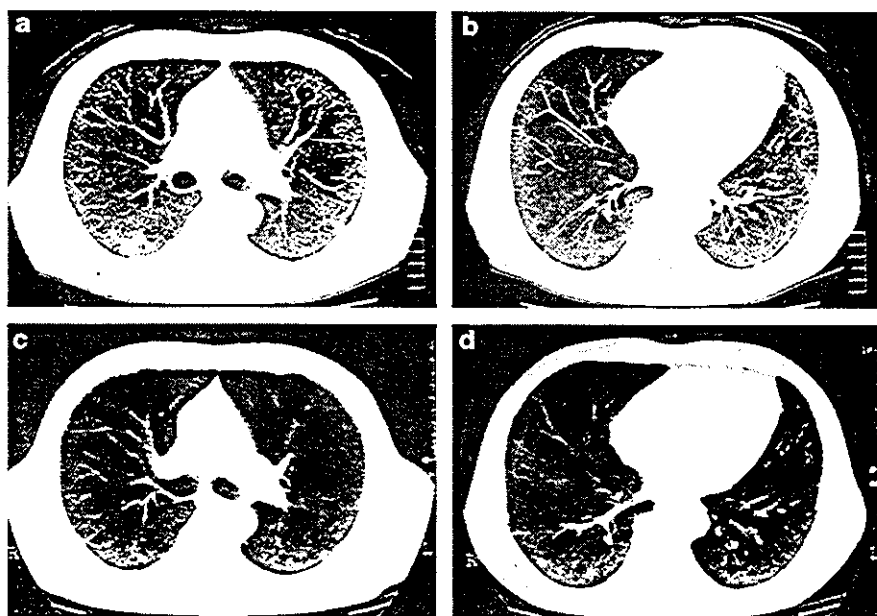
Figure 1 Chest CT performed before initiation and after cessation of imatinib mesylate. CT scans obtained at the level of bronchus intermedius (a) and lung bases (b) revealed reticular shadow and ground-glass opacities at subpleural area in both lung. CT scans obtained 18 days after discontinuation of imatinib mesylate at the level of bronchus intermedius (c) and lung bases (d) revealed that reticular shadow and ground-glass opacities almost disappeared.
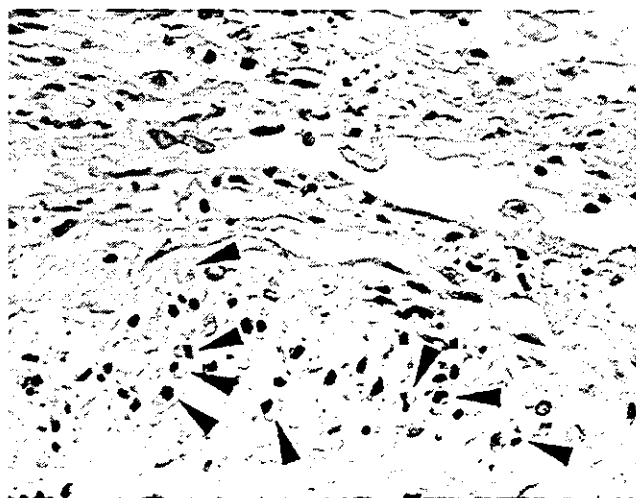
Figure 2 Pathological findings of transbrochial lung biopsy. Alveolar structures were destroyed in most of the microscopic field in the TBLB specimen. Prominent infiltration of eosinophilic leukocytes (indicated by arrows) was observed in loose fibrous tissue. These findings are compatible with drug-induced interstitial pneumonia. (H–E stain, × 400).

lacked pathologic corroboration.[4] Recently, Rosado et al[5] also reported a case of imatinib-induced interstitial pneumonia diagnosed by TBLB, but whose pathological findings were compatible with the nonspecific interstitial pneumonia without eosinophilic infiltration. The above data, taken together with our observations, suggest that imatinib-induced interstitial pneumonia may be heterogeneous and some of them may be likely to

involve an immunoallergic mechanism. So far, the frequency of interstitial pneumonia related to imatinib appears to be relatively low and the underlying mechanism is still unclear; however, we must pay close attention to this adverse event.

T Yokoyama[1]
K Miyazawa[1]
E Kurakawa[1]
A Nagate[1]
T Shimamoto[1]
K Iwaya[2]
S Akata[3]
M Aoshima[1]
H Serizawa[2]
K Ohyashiki[1]

[1]First Department of Internal Medicine, Tokyo Medical University, Japan;
[2]Division of Surgical Pathology, Tokyo Medical University, Japan; and
[3]Department of Radiology, Tokyo Medical University, Japan

References

1 O'Brien SG, Guilhot F, Larson RA, Gathmann I, Baccarani M, Cervantes F et al. IRIS investigators: imatinib compared with interferon low-dose cytarabine for newly diagnosed chronic-phase chronic myeloid leukemia. N Engl J Med 2003; 348: 994–1004.
2 Hehlmann R. Current CML therapy: progress and dilemma. Leukemia 2003; 17: 1010–1012.
3 Kantarjian H, Sawyers C, Hochhaus A, Guilhot F, Schiffer C, Gambacorti-Passerini C et al. International STI571 CML Study Group: hematologic and cytogenetic responses to imatinib mesylate in chronic myelogenous leukemia. N Engl J Med 2002; 346: 645–652.
4 Bergeron A, Bergot E, Vilela G, Ades L, Devergie A, Esperou H et al. Hypersensitivity pneumonitis related to imatinib mesylate. J Clin Oncol 2002; 20: 4271–4272.
5 Rosado MF, Donna E, Ahn YS. Challenging problems in advanced malignancy: case 3. Imatinib mesylate-induced interstitial pneumonitis. J Clin Oncol 2003; 21: 3171–3173.

Stromal cell–derived factor-1α/CXCL12–induced chemotaxis of T cells involves activation of the RasGAP-associated docking protein p62Dok-1

Seiichi Okabe, Seiji Fukuda, Young-June Kim, Masaru Niki, Louis M. Pelus, Kazuma Ohyashiki, Pier Paolo Pandolfi, and Hal E. Broxmeyer

Events mediating stromal cell–derived factor-1 (SDF-1α/CXCL12) chemotaxis of lymphocytes are not completely known. We evaluated intracellular signaling through RasGAP-associated protein p62Dok-1 (downstream of tyrosine kinase [Dok-1]) and associated proteins. SDF-1α/CXCL12 stimulated Dok-1 tyrosine phosphorylation and association with RasGAP, adaptor protein p46Nck, and Crk-L in Jurkat T cells. The phosphorylation of Dok-1 was blocked by pretreatment of cells with the src kinase inhibitor PP2. Src kinase family member Lck was implicated. SDF-1α/CXCL12 did not phosphorylate Dok-1 in J.CaM1.6 cells, a Jurkat derivative not expressing Lck, but did phosphorylate Dok-1 in J.CaM1.6 cells expressing Lck. SDF-1α/CXCL12 induced the tyrosine phosphorylation of Pyk2 and the association of Pyk2 with zeta chain–associated protein-70 kilodaltons (Zap-70) and Vav. SDF-1α/CXCL12 enhanced the association of RasGAP with Pyk2. CXCR4-expressing NIH3T3 and Baf3 cells transfected with full-length Dok-1 cDNA were suppressed in their responses to SDF-1α/CXCL12–induced chemotaxis; mitogen-activated protein (MAP) kinase activity was also decreased. Chemotaxis to SDF-1/CXCL12 was significantly enhanced in Dok-1⁻/⁻ CD4⁺ and CD8⁺ splenic T cells. These results implicate Dok-1, Nck, Crk-L, and Src kinases—especially Lck, Pyk2, Zap-70, Vav, and Ras-GAP—in intracellular signaling by SDF-1α/CXCL12, and they suggest that Dok-1 plays an important role in SDF-1α/CXCL12–induced chemotaxis in T cells. (Blood. 2005;105:474-480)

© 2005 by The American Society of Hematology

Introduction

Chemokines play a central role in lymphocyte trafficking and homing. The chemokine stromal cell–derived factor-1α (SDF-1α/CXCL12) binds to CXC chemokine receptor 4 (CXCR4).[1,2] CXCR4 is a 7-transmembrane surface structure linked to G proteins.[3] CXCR4 is expressed on a number of cell types, including T cells, hematopoietic stem cells, and progenitor cells. SDF-1α/CXCL12 is a highly efficient chemoattractant for T lymphocytes and other cells. Targeted disruption of SDF-1α/CXCL12 or CXCR4 is lethal in mice and is associated with the absence of lymphoid and myeloid hematopoiesis in the fetal bone marrow.[4,5]

The p120RasGAP-associated p62 protein Dok-1 (downstream of tyrosine kinase) was originally defined as a tyrosine-phosphorylated 62-kDa protein that coimmunoprecipitated with p21Ras GTPase-activating protein (RasGAP).[6] Dok-1 is a docking protein purified from v-Abl or BCR-Abl–transformed hematopoietic cells. It consists of pleckstrin homology (PH) and phosphotyrosine binding (PTB) domains in the amino-terminal and the tyrosine phosphorylation site.[7] Dok-1 is tyrosine phosphorylated by several cytokines, such as kit-ligand, platelet-derived growth factor (PDGF), and vascular endothelial growth factor (VEGF), and couples with the cytoplasmic protein tyrosine kinase (PTK).[8,9] Dok-1 is considered to be a downstream target of PTKs and to play a negative role in various signaling pathways.[10]

RasGAP is an essential component of Ras-activated signaling pathways. RasGAP has GTPase stimulating activity in the carboxy-terminus and has 2 src homology domains (SH2) and 1 SH3 domain in the amino-terminal region. RasGAP down-regulates Ras activity, converting the activate form of RasGTP to the inactive form, RasGDP, and it plays a role in cell growth and differentiation.[11,12]

Proline-rich tyrosine kinase 2 (Pyk2), also known as cellular adhesion kinase β (CAKβ), related adhesion focal tyrosine kinase (RAFTK), and calcium-dependent tyrosine kinase (CADTK) are predominantly expressed in cells derived from hematopoietic lineages and in the central nervous system.[13-16] Pyk2 is one of the signaling mediators critical for signaling through G protein–coupled receptors, is activated by signals that elevate intracellular calcium concentrations, and is required for activation of mitogen-activated protein kinase (MAPK) signaling. Pyk2 is tyrosine phosphorylated after T-cell receptor (TCR) stimulation.[17,18]

The aims of our study were to evaluate intracellular effects mediating the chemotaxis induced by SDF-1α/CXCL12 and to determine whether this intracellular signaling pathway involved Dok-1, RasGAP, or Pyk2. Our results suggest that Dok-1, RasGAP, and Pyk2 are involved in SDF-1α/CXCL12 signaling.

Materials and methods

Reagents and antibody

Recombinant human SDF-1α/CXCL12, antiphosphotyrosine monoclonal antibody (mAb; 4G10) and anti–Crk-L mAb were purchased from Upstate

Biotechnology (Lake Placid, NY). Rabbit anti–Dok-1 antibody (Ab), agarose-conjugated goat anti–Dok-1 Ab, anti-RasGAP mAb, anti-Vav Ab, phopho-ERK1 Ab, and protein A/G agarose were obtained from Santa Cruz Biotechnology (Santa Cruz, CA). Rabbit anti–Dok-1 Ab was purchased from Prosci Incorporated (Poway, CA). Antiphosphotyrosine mAb (PY20), anti-Pyk2 mAb, and anti-Nck mAb, and anti–Zap-70 mAb were obtained from Transduction Laboratories (Lexington, KY). Src kinase inhibitor PP2 was obtained from Calbiochem-Novabiochem (San Diego, CA). Anti-CXCR4 mAb was from R&D Systems (Minneapolis, MN). Other reagents were from Sigma (St Louis, MO).

Construction of plasmid

The plasmid encoding mouse dok-1 was kindly provided by Dr Y. Yamanashi (Tokyo University, Japan). The complementary DNA (cDNA) encoding full-length dok-1 was amplified by polymerase chain reaction and was cloned into a mammalian GFP-expressing vector, GFP Fusion TOPO TA Expression Kits (Invitrogen, Carlsbad, CA), or a retroviral vector (pQCXIR; Clontech, Palo Alto, CA) at the NotI/PswI site.

Cell culture, transfection, and infection

Human leukemic T-cell line Jurkat, Lck-deficient T-cell line J.CaM1.6, and J.CaM1.6 cells engineered to express Lck were maintained in RPMI 1640 medium supplemented with 10% heat-inactivated fetal bovine serum (FBS) with 1% penicillin/streptomycin in a humidified incubator at 37°C. Murine fibroblast NIH3T3 cells expressing human CXCR4 and CD4 were maintained in Dulbecco modified Eagle minimal medium (DMEM) supplemented with 2 mM L-glutamine and 1% penicillin/streptomycin. Transfections were performed using LipofectAMINE 2000 (Invitrogen) according to the manufacturer's protocol. After transfection, cells were sorted using flow cytometry and were used for chemotaxis assay. For retroviral production, Phoenix-echo cells were transfected with empty vector alone or with full-length dok-1 using LipofectAMINE 2000 (Invitrogen). Supernatant was collected 24 hours and 48 hours after transfection. NIH3T3 cells were infected using supernatant and were analyzed by Western blot. Murine IL-3–dependent cell line Baf-3 and Dok-1–transfected Baf-3 Dok cells were cultured with 10% fetal calf serum (FCS) RPMI 1640 with 0.1 ng/mL murine interleukin-3 (IL-3). Lck cDNA expressing J.CaM/Lck cells were kind gifts from A. Weiss (University of California, San Francisco) and were cultured with 10% FCS RPMI 1640.

Immunoprecipitation and Western blot analysis

Jurkat, J.CaM1.6, and NIH3T3 cells were factor starved overnight and treated with 100 ng/mL SDF-1α/CXCL12, a predetermined optimal concentration, at the indicated times and were washed once with ice-cold phosphate-buffered saline (PBS). Cells were lysed in lysis buffer containing 20 mM Tris-HCl, pH 8.0, 137 mM NaCl, 10% glycerol, 1 mM phenylmethylsulfonyl fluoride (PMSF), 10 μM ethylenediaminetetraacetic acid (EDTA), 10 μg/mL leupeptin, 100 mM sodium fluoride, 2 mM sodium orthovanadate, and 1% NP-40 for 20 minutes on ice. Lysates were centrifuged at 12 000 rpm (10 000 × g) for 20 minutes at 4°C. The protein content of lysates was determined with a protein assay kit (Bio-Rad Laboratories, Hercules, CA). Equivalent amounts of protein in cell lysates were boiled with 2 × SDS (sodium dodecyl sulfate) sample buffer for 5 minutes. For immunoprecipitation, cell lysates were incubated at 4°C overnight with the indicated precipitating antibody. Immunoprecipitates were collected using 40 μL protein A/G-agarose for 2 hours at 4°C. After 4 washings in lysis buffer, immunocomplexes were eluted and boiled for 5 minutes in 2 × sample buffer. Proteins or immunocomplexes were loaded onto polyacrylamide gels (BioWhittaker, Walkersville, MD) and then were transferred to polyvinylidene difluoride (PVDF) membranes (Millipore, Bedford, MA). The membranes were blocked by 3% skim milk, PBS-Tween 20 (PBST) or 1% bovine serum albumin (BSA) PBST and probed with the indicated primary antibody at appropriate dilutions for 2 hours at room temperature (RT) or overnight at 4°C. Blots were probed with secondary antibody–conjugated horseradish peroxidase, and were developed using the enhanced chemiluminescence (ECL; Amersham Phamacia Biotech, Bucks, United

Kingdom) system with ECL film according to the manufacturer's specification.

Chemotaxis assay

Chemotaxis assays for Jurkat, J.CaM1.6, and NIH3T3 cells were performed with 48-well microchemotaxis chambers with 8-μm pore size polycarbonate filters (NeuroProbe, Gaithersburg, MD). Filters were soaked overnight in 0.1% wt/vol gelatin solution (Sigma). The chemotaxis medium (0.2% BSA in DMEM with and without 100 ng/mL SDF-1α/CXCL12) was placed in the lower chamber, and 50 μL cell suspension (1.6 × 10^5 cells/mL) in chemotaxis medium (without SDF-1α/CXCL12) was placed in the upper wells. After incubation of the apparatus at 37°C for 3 to 4 hours in humidified air with 5% CO_2, filters were removed, fixed, and stained with the use of DiffQuik staining kit (Dade Behring, Newark, DE). Cells were counted in 3 high-power fields (HPFs; 400 ×). Results were expressed as the mean number of migrating cells in 1 HPF.

Transmigration assay of splenic T cells

Splenic T cells from Dok−/− and control mice[19] were isolated by negative selection using the pan T-cell isolation kit (Miltenyi Biotech, Auburn, CA), which depletes cells expressing B220, Gr-1, and Ter119. The purity of T cells was evaluated by staining CD4 and CD8 and was greater than 95%. The chemotaxis assay to SDF1α/CXCL12 in the face of positive, negative, and zero gradient was performed as described.[20] After a 4-hour migration assay, input cells and cells that migrated to the bottom chamber were enumerated and stained with fluorescein isothiocyanate (FITC)–conjugated anti-CD4 and phycoerythrin (PE)–conjugated anti-CD8 antibodies (BD Biosciences, San Diego, CA) to determine the migration of T-cell subsets by flow cytometry. Migration index was calculated by the number of cells migrated divided by the background migration without SDF1α/CXCL12. Expression of CXCR4 was determined by staining the isolated T cells with biotinylated antimouse CXCR4 mAb (clone 2B11/CXCR4; BD Biosciences) with or without anti-CD4 and anti-CD8 Abs, followed by cytochrome-conjugated streptavidin staining.

Flow cytometric analysis

NIH3T3 cells were detached by incubation with 10 mM EDTA in DMEM for 10 minutes, transferred to tubes, and sedimented (10 000 rpm, 1 minute [7000 × g]). Cells were stimulated with 100 ng/mL SDF-1α/CXCL12 at 37°C for the indicated times, washed once in ice-cold PBS, and fixed using the Cytofix/Cytoperm kit (BD PharMingen, San Diego, CA) or 1% paraformaldehyde PBS. Cells were incubated with phospho-Erk1 Ab for 1 hour and then incubated with phycoerythrin (PE)–conjugated secondary antibody. MAPK activities were monitored by flow cytometric analysis, and data obtained from 5 independent measurements were evaluated with the Student t test. To evaluate cell surface CXCR4, cells were fixed with 1% paraformaldehyde PBS and incubated with anti-CXCR4 mAb. Cell were stained with FITC-conjugated secondary antibody and analyzed by flow cytometry.

Results

SDF-1α/CXCL12 induces tyrosine phosphorylation of Dok-1 and the association of Dok-1 with RasGAP, Nck, and Crk-L

Dok-1 is activated by different proteins, such as CD2.[21] To characterize signaling pathways activated by SDF-1α/CXCL12, we used the Jurkat T-cell line, which expresses the SDF-1α/CXCL12 receptor CXCR4. Jurkat cells were stimulated with 100 ng/mL SDF-1α/CXCL12 or control medium for 5 minutes. Cell lysates were subjected to anti–Dok-1 immunoprecipitation and to immunoblotting with antiphosphotyrosine antibody (Figure 1A). SDF-1α/CXCL12 stimulated the tyrosine phosphorylation of Dok-1. Nck is a ubiquitously expressed protein composed entirely of a single SH2 and 3 SH3 domains that fit into the adaptor class of
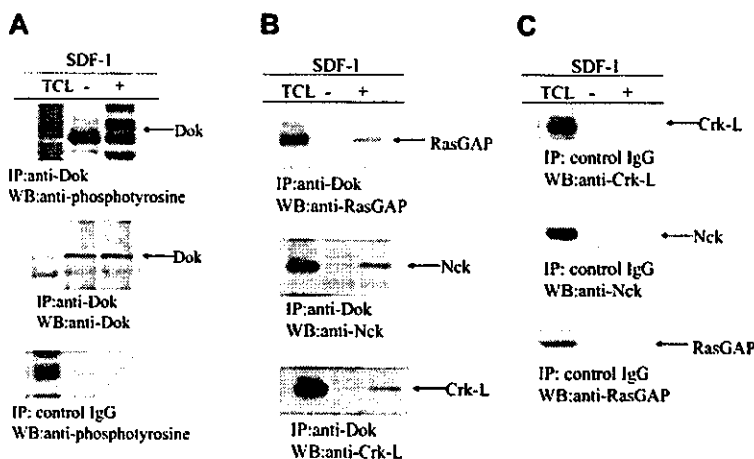
Figure 1. Dok-1 is tyrosine phosphorylated and associates with RasGAP, Nck, and Crk-L after SDF-1α/CXCL12 stimulation. (A) Jurkat cells were left unstimulated (−) or stimulated with SDF-1α/CXCL12 (100 ng/mL) for 5 minutes. Total cell lysates (TCLs) were immunoprecipitated with anti–Dok-1 Ab. Immunoprecipitates (IPs) were immunoblotted with antiphosphotyrosine antibody (upper panel) or anti–Dok-1 Ab (middle panel). As control, IPs were made with control IgG, and immunoblotting was performed with antiphosphotyrosine antibody (lower panel). (B) Immunoprecipitates were immunoblotted with anti-RasGAP, Nck, and Crk-L antibodies. (C) As a control for panel B, IPs with control IgG Ab were immunoblotted with anti-RasGAP, anti-Nck, or anti–Crk-L Abs. (A-C) Results are representative of at least 3 experiments. WB indicates Western blot.

signaling molecules.[22] Crk-L is in the family of Crk adaptor proteins and was discovered in the form of an oncogene carried by 2 sarcoma-inducing retroviruses.[23,24] Crk-L and Crk play a role in the signaling pathways of the T-cell receptor.[25,26] Dok-1 associates with RasGAP and the adaptor proteins Nck and Crk-L after stimulation.[27,28] To determine whether SDF-1α/CXCL12 induces the association of such molecules, coimmunoprecipitation experiments were performed. SDF-1α/CXCL12 triggering induced significant association of Dok-1 with RasGAP, Nck, and Crk-L (Figure 1B). Tyrosine phosphorylation of SDF-1/CXCL12–stimulated cells was not seen when control immunoglobulin G (IgG) was used for immunoprecipitation (Figure 1A, lower panel), and neither CrK-L, NcK, nor RasGAP was detected in control IgG immunoprecipitates (Figure 1C).

SDF-1α/CXCL12–induced Dok-1 tyrosine phosphorylation depends on Src kinase activity

Dok-1 protein is phosphorylated by a wide range of PTKs, and Src family kinases are involved in SDF-1α/CXCL12 signaling.[29] We tested the potential relationships of Src to Dok-1 for SDF-1/CXCL12 signaling by using the specific Src kinase inhibitor, PP2. Jurkat cells were pretreated with 10 μM PP2 for 30 minutes and then were stimulated with SDF-1α/CXCL12. Pretreatment of Jurkat cells with PP2 completely blocked Dok-1 phosphorylation (Figure 2A). PP2 was not toxic to Jurkat cells, as assessed by trypan blue exclusion and cell numbers (data not shown). Using GST fusion proteins, we found that Dok-1 directly binds to the src kinase family members, Fyn and Lck, after SDF-1α/CXCL12 stimulation but does not bind without SDF-1/CXCL12 treatment (Figure 2B). Lck regulates T-cell surface receptors, such as CD2 and CD4.[30,31] We used J.CaM1.6 cells, a derivative of Jurkat cells that are defective in Lck, to determine whether Lck played a role in the activation of Dok-1. Dok-1 phosphorylation was completely blocked in J.CaM1.6 cells (Figure 2C), but not in J.CaM1.6 cells engineered to express Lck (Figure 2D), in response to SDF-1α/CXCL12 (Figure 2C), suggesting that Lck is involved in the regulation of Dok-1 phosphorylation in J.CaM1.6 cells in response to SDF-1α/CXCL12. Cell surface expression of CXCR4 was not different between J.CaM1.6 cells and the parental Jurkat cells (Figure 2E), demonstrating that differences between the 2 cell lines were not attributed to surface expression of CXCR4.

SDF-1α/CXCL12 induces tyrosine phosphorylation of Pyk2, and Pyk2 association with Zap-70 and Vav

Pyk2 is expressed mainly in the central nervous system and in cells derived from hematopoietic lineages. Pyk2 is activated by a variety
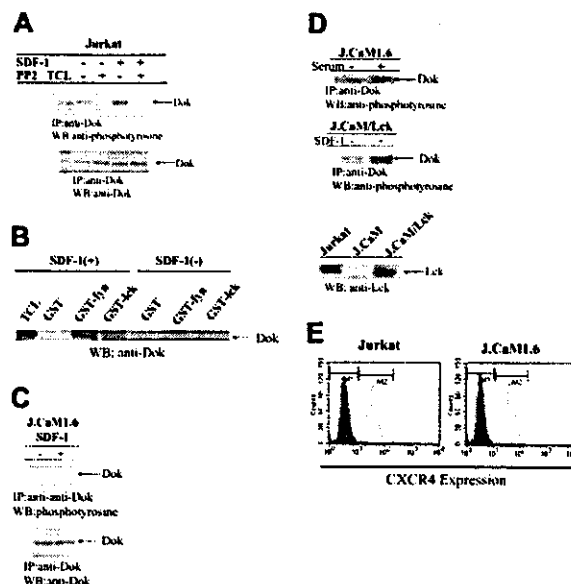
Figure 2. Dok-1 phosphorylation in response to SDF-1α/CXCL12 is blocked by src kinase inhibitor PP2, and Dok-1 is not phosphorylated in the Lck-deficient T-cell line J.CaM1.6. (A) Jurkat cells were pretreated with src kinase inhibitor PP2 (10 μM) for 30 minutes and were left unstimulated or stimulated with SDF-1α/CXCL12 at 100 ng/mL for 5 minutes. Cell lysates were immunoprecipitated with anti–Dok-1 Ab and were immunoblotted with antiphosphotyrosine (top panel) or anti–Dok-1 Ab (bottom panel). (B) Cells were stimulated with or without SDF-1, and cell lysates were incubated with agarose-conjugated GST, GST-fyn, or GST-lck and immunoblotted with anti-Dok Ab. (C) Total cell lysates from J.CaM1.6 cells were immunoprecipitated with anti–Dok-1 Ab and then immunoblotted with antiphosphotyrosine (top panel) or anti–Dok-1 Ab (bottom panel). (D) J.CaM1.6 cells were unstimulated or stimulated with serum. Cell lysates were incubated with anti-Dok Ab and were immunoblotted with antiphosphotyrosine Ab (top panel). J.CaM1.6 cells were unstimulated or stimulated with SDF-1. Cell lysates were incubated with anti-Dok Ab and immunoblotted with antiphosphotyrosine Ab (middle panel). Cell lysates of Jurkat, J.CaM1.6, and J.CaM/Lck were immunoblotted with anti-Lck Ab (bottom panel). (E) CXCR4 expression on Jurkat and J.CaM1.6 cells. Cells were fixed with 1% paraformaldehyde PBS. Cells were incubated with anti-CXCR4 mAb or normal mouse IgG and were stained with FITC-conjugated secondary Ab and analyzed by flow cytometry. (A-E) Results in each panel are representative of at least 3 experiments each.

of extracellular signals that elevate intracellular calcium concentration and by stress signals.[13,16] Phosphorylation of Pyk2 leads to the recruitment of src family kinases and activation of ERKs.[13,15] We evaluated a role for Pyk2 in SDF-1α/CXCL12 signaling. Pyk2 was tyrosine phosphorylated after SDF-1α/CXCL12 stimulation, without an effect on the total amount of Pyk2 (Figure 3A). Vav is a hematopoietic cell-specific guanine nucleotide exchange factor for small guanosine triphosphate (GTP)–binding proteins.[32] Zap-70 is a PTK that associates with the ζ subunit of the TCR. Zap-70 is tyrosine phosphorylated after TCR stimulation.[33,34] As seen in Figure 3B, tyrosine-phosphorylated Pyk2 associates with Vav and Zap-70 after SDF-1α/CXCL12 stimulation.

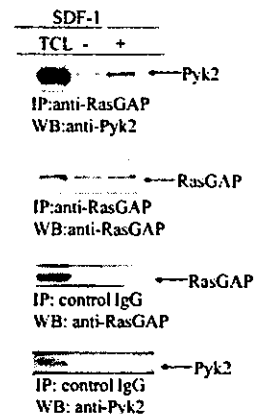### SDF-1α/CXCL12 induces RasGAP association with Pyk2

RasGAP is an essential component of Ras-activated signaling pathways and down-regulates Ras activity. The association of RasGAP with Pyk2 was enhanced after SDF-1α stimulation (Figure 4). This suggests that RasGAP association with Pyk2 is involved in SDF-1α/CXCL12 signaling.

Overexpression of Dok-1 interferes with cell migration of CXCR4-expressing NIH3T3 and Baf3 cells and regulates MAPK activity in NIH3T3 cells

We demonstrated that Dok-1 associates with the adaptor proteins Nck and Crk-L (Figure 1B). Because Nck and Crk-L are involved in cell migration to SDF-1α/CXCL12,[35,36] we studied whether overexpression of Dok-1 influenced chemotaxis of CXCR4-expressing NIH3T3 and Baf3 cells in response to SDF-1α/CXCL12. Dok-1 cDNA was transfected to NIH3T3 cells expressing human CXCR4. Surface CXCR4 expression levels were not different between the parental CXCR4-expressing NIH3T3 cells
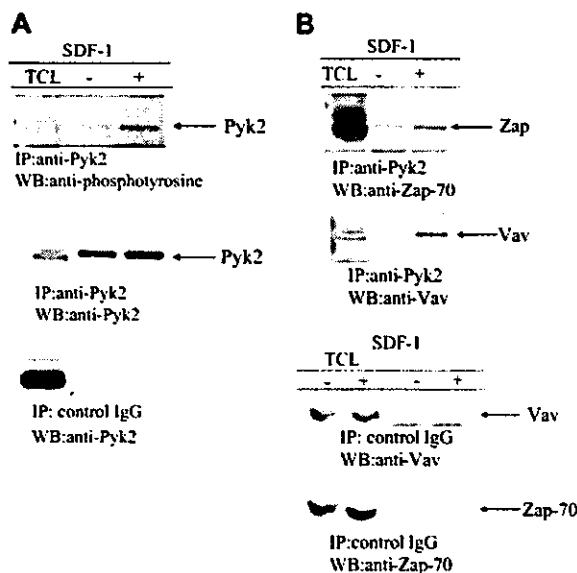
Figure 3. Pyk2 is tyrosine phosphorylated and associates with Zap-70 and Vav in Jurkat cells in response to SDF-1α/CXCL12. Cells were treated without and with SDF-1/CXCL12. (A) Pyk2 was immunoprecipitated from cell lysates of nonstimulated or SDF-1α/CXCL12–stimulated cells and was analyzed by Western blotting with antiphosphotyrosine (bottom panel) and Pyk2 (middle panel). As a control, control IgG–immunoprecipitated lysates were immunoblotted with anti-Pyk2 Ab (bottom panel). (B) Anti-Pyk2 (top two panels) or control IgG (bottom two panels) immunoprecipitates were immunoblotted with anti-Zap-70 or Vav Ab. (A-B) Results are representative of at least 3 experiments.

Figure 4. SDF-1α/CXCL12 induces RasGAP association with Pyk2 in Jurkat cells. RasGAP immunoprecipitates were analyzed by Western blotting with anti-Pyk2 or anti-RasGAP Ab. Shown are results of 1 of 3 representative experiments. IP controls for RasGAP and Pyk2 are shown in the bottom two panels. The total amount of Pyk2 did not change after treatment with SDF-1, similar to the results noted in Figure 3A.

transfected with empty vector and their dok-1 cDNA–transfected counterparts, as determined by flow cytometry and Western blot analysis (Figure 5A-B). Dok-1 overexpressing NIH3T3 cells were significantly decreased in response to SDF-1α/CXCL12–induced chemotaxis compared with empty vector–transfected NIH3T3 cells (Figure 5Ci). Baf3 cells and Baf3 cells overexpressing Dok-1 express similar levels of CXCR4 (data not shown). As seen in Figure 5Cii, Baf3 cells overexpressing Dok-1 were significantly suppressed in their chemotactic response to SDF-1/CXCL12. Dok-1 is considered a negative regulator of cell proliferation and Ras/MAPK signaling pathways.[10] To evaluate Dok-1 regulation of MAPK activity after SDF-1α/CXCL12 signaling, we used Dok-1–overexpressing NIH3T3 cells (Figure 5D-E). Dok-overexpressing NIH3T3 cells manifested reduced MAPK activity (Figure 5D) and decreased phosphorylation of Erk1 (Figure 5E) in response to SDF-1α/CXCL12 compared with mock-transfected cells. This suggests that Dok-1 plays a role in SDF-1α/CXCL12–induced chemotaxis and regulation of MAPK activity.

To determine the relevance and importance of Dok-1 in SDF-1/CXCL12–induced chemotaxis, we evaluated the chemotactic responses of T-lymphocyte subsets from the spleens of Dok-1^{−/−} and Dok-1^{+/+} mice[19] to graded amounts of SDF-1/CXCL12. As shown in Figure 6, total T cells, CD4^{+} T cells, and CD8^{+} T cells from the spleens of Dok-1^{−/−} mice were enhanced in their chemotactic response to SDF-1/CXCL12; maximum enhancement occurred for Dok-1^{−/−} T cells at a concentration of SDF-1/CXCL12 that maximally stimulated chemotaxis for Dok-1^{+/+} T cells. Chemotaxis of Dok-1^{−/−} and Dok-1^{+/+} T cells to SDF-1CXCL12 was blocked by placing SDF-1/CXCL12 in the upper chamber or in both the upper and the lower chambers, demonstrating that the effects seen (migration to the lower chamber) were caused by chemotaxis and not by chemokinesis. Differences in chemotactic responses of Dok-1^{−/−} and Dok-1^{+/+} T cells to SDF-1/CXCL12 were not caused by differences in levels of expression of CXCR4 (Figure 6B). These results demonstrate that Dok-1 negatively regulates primary T-cell chemotaxis to SDF-1/CXCL12. Along with the data shown (Figure 5A, Ci-ii), Dok-1 may also negatively regulate the migration of other cell types to SDF-1/CXCL12.
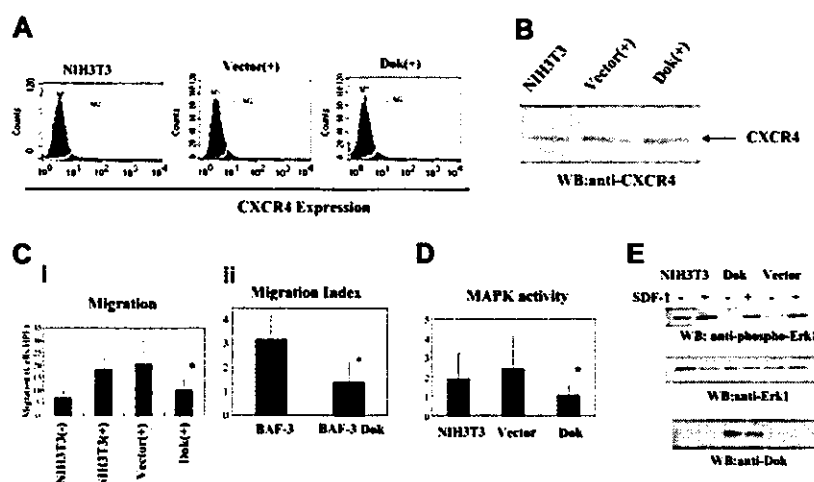
Figure 5. Influence of Dok-1 overexpression on SDF-1α/CXCL12-induced chemotaxis and activation of MAPK activity. (A) CXCR4 expression on NIH3T3 cells transfected with GFP-tagged full-length Dok-1 or with empty vector. Dok or vector-transfected NIH3T3 cells were incubated with anti-CXCR4 Ab or normal mouse IgG, stained with FITC-conjugated secondary Ab, and analyzed by flow cytometry. (B) CXCR4 protein from cell lysates of Dok or vector-transfected cells as assessed after immunoblotting with anti-CXCR4 Ab. (C) Chemotaxis in response to SDF-1α/CXCL12. (Ci) NIH3T3 cells were transfected with GFP-tagged full-length Dok-1 or with empty vector. Cell migration was analyzed in 48-well chemotaxis chambers. After sorting GFP+ cells, 8000 cells were placed in the upper chambers. Three to 4 hours later, cells were stained using the DiffQuik kit, and the migrating cells were counted under high-power fields (× 400). Data represent the arithmetic mean ± SEM of 4 experiments. *P < .05 compared with control vector. (Cii) Baf3 cells were transfected with full-length Dok-1. Cell migration was analyzed with chemotaxis chambers. Cells (2 × 10⁵) input cells were placed in the upper chamber, and migrated cells were counted by fluorescence-activated cell sorter (FACS). Data represent the arithmetic mean ± SEM of 3 experiments. (D) MAPK activity. NIH3T3 cells were transfected with expression vector encoding Dok-1 or empty vector. Cells were stimulated with or without SDF-1α/CXCL12. Cells were fixed and stained with phospho-ERK1 Ab. MAPK activity was analyzed by flow cytometry. Data represent the arithmetic mean ± SEM of 5 experiments. *P < .05 compared with control vector. (E) Phosphorylation of ERK-1. Dok or vector-transfected NIH3T3 cells were stimulated with SDF-1/CXCL12. Cell lysates were immunoblotted with anti-phospho Erk-1 Ab, Erk-1 Ab, or Dok Ab. Data represent results of 1 of 3 similar experiments.

Discussion

Chemokines belong to a large family of chemoattractant molecules and have been implicated in a number of different functions mediated through chemokine receptors. SDF-1α/CXCL12 plays a role in regulating the migration and homing of hematopoietic cells and is a highly efficient chemotactic factor for T cells. Several studies have evaluated the intracellular molecules involved in SDF-1α/CXCL12-induced chemotaxis of cells. In T cells, SDF-1α/

CXCL12 stimulation results in activation of the Janus kinase/signal transduction and activation of transcription (Jak/STAT) pathways.[34] Phosphatidylinositol 3-kinase (PI3-K), Crk-associated substrate (p130Cas), focal adhesion kinase (FAK), and protein kinase C (PKC) are activated by SDF-1α/CXCL12,[35] but the signaling mechanisms involved are not yet fully determined. Our present report implicates the docking protein, Dok-1, as a mediator of SDF-1α/CXCL12-induced migration of T cells and associated intracellular signals; Dok-1 links with downstream effectors of SDF-1α/CXCL12/CXCR4 signaling. Dok-1 has typical features of
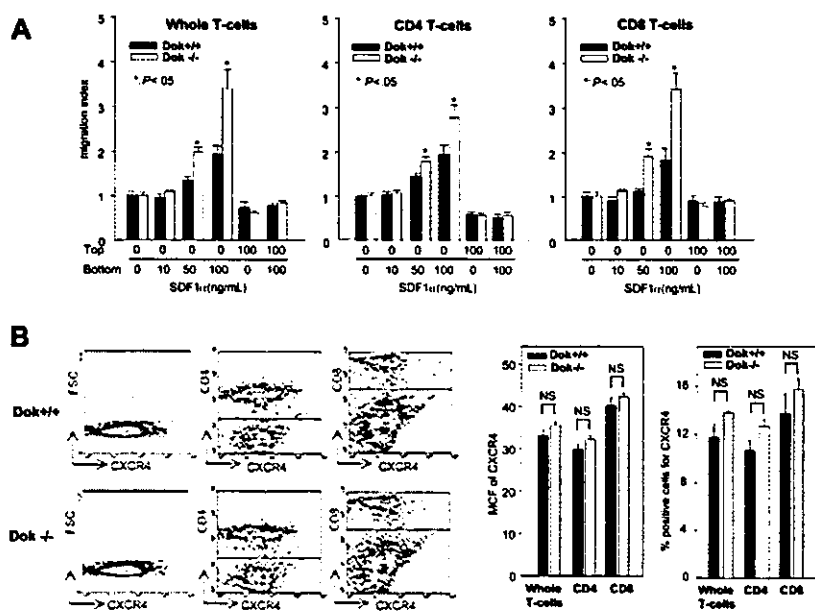
Figure 6. Migration to SDF-1α and CXCR expression of splenic T cells from control or Dok−/− mice. Half a million purified T cells from Dok−/− or control (Dok+/+) mice were subjected to migration assay in a positive gradient of escalating doses of recombinant murine (rm) SDF-1α and a negative gradient and zero gradient of 100ng/mL of SDF-1α. After 4-hour migration, cells were enumerated by flow cytometry. (A) Input cells and migrated cells were stained with anti-CD4 and anti-CD8 antibodies to determine the numbers of CD4 and CD8 cells migrated. Migration index of whole, CD4, and CD8 cells are shown. Data are expressed as mean ± SEM from 6 mice of each group for CD4 cells (2 experiments with 3 mice each) and 3 mice of each group for whole or CD8 migration (*P < .05 compared with control cells. (B) Isolated T cells were stained with anti-CXCR4 and anti-CD4 or anti-CD8 antibodies. (left) Result of 1 representative experiment. (right) Percentage of positive cells and mean channel fluorescence (MCF) for CXCR4. Data are mean ± SEM of 3 mice per group for 1 experiment. NS indicates not significant.

multiadaptor proteins, such as a membrane localization sequence (PH domain), receptor interaction domain (PTB domain), and several putative binding sites for downstream substrates (phospho-tyrosine and PXXP elements). Dok-1 was identified as a tyrosine-phosphorylated protein of 62-kDa associated with p120RasGAP in fibroblasts transfected with v-src.[6] Dok-1 is phosphorylated by several receptor tyrosine kinases and is regulated by tyrosine kinase. Src family kinases, such as Src, Fyn, and Lck, regulate Dok-1 phosphorylation.[21] Lck is required for CD2-mediated phosphorylation of Dok-1. We have shown that Dok-1 tyrosine phosphorylation is completely blocked by use of the specific src kinase inhibitor PP2, implicating a reliance of Dok-1 on src family kinases (Figure 2A). We also found that Dok-1 phosphorylation was completely blocked after SDF-1α/CXCL12 stimulation in the Lck-deficient T-cell line J.CaM1.6 (Figure 2C), but not in J.CaM1.6 cells engineered to express LcK (Figure 2D), demonstrating that Lck regulates Dok-1 phosphorylation in this T-cell line.

Coimmunoprecipitation studies demonstrated that tyrosine-phosphorylated Dok-1 binds directly to RasGAP, Nck, and Crk-L. We had previously reported Nck involvement in SDF-1α/CXCL12 signaling and chemotaxis in Jurkat cells,[37] thereby implicating RasGAP, Nck, and CrK-L in SDF-1α/CXCL12–induced cell chemotaxis. To study the role of Dok-1 regulation of cell migration and MAPK activity in response to SDF-1α/CXCL12, Dok-1 cDNA was transfected into NIH3T3 cells expressing human CXCR4 and Baf3, which express CXCR4. Dok-1–transfected NIH3T3 and Baf3 cells were significantly less responsive to SDF-1α/CXCL12-induced chemotaxis than empty vector–transfected cells, directly demonstrating Dok-1 as one of the intracellular molecules involved in SDF-1α/CXCL12–induced migration. Analysis of Dok-1 knock-out mice reveals that Dok-1 is a negative regulator of cell proliferation.[10] Cells derived from Dok-1 knockout mice hyperpro-

liferate in response to a number of cytokines and growth factors. Moreover, we found that total T cells, as well as CD4+ T cells and CD8+ T cells, from the spleens of Dok-1−/− mice were enhanced in response to SDF-1/CXCL12–induced chemotaxis compared with Dok-1+/+ T cells (Figure 6). Dok-1 negatively regulates MAPK activity in T cells. We also found that Dok-1 regulates MAPK activity in response to SDF-1α/CXCL12 signaling (Figure 5D-E).

Pyk2 is a non–receptor tyrosine kinase belonging to the focal adhesion kinase family. Pyk2 interacts with several signaling intermediates. Pyk2 has no SH2 or SH3 domains, but it is proposed that proline-rich stretches in the C-terminus act as ligands for SH3 domain–containing signaling proteins. Pyk2 is constitutively expressed in human T cells and is rapidly phosphorylated on the activation of TCR. This is associated with its increased association with Src and Grb2.[17,18] We found that Pyk2 is tyrosine phosphory-lated after SDF-1α/CXCL12 stimulation in Jurkat cells. Moreover, the present data also show that Pyk2 associates with Zap-70 and Vav. Pyk2 has been shown to participate in the activation of MAPKs. RasGAP is implicated as a negative regulator of ras because it is capable of stimulating the intrinsic GTPase-inactive guanosine diphosphate (GDP)–bound form of the molecule. Inter-estingly, Pyk2 can bind to RasGAP after SDF-1α/CXCL12 stimula-tion. Thus, Pyk2 also appears to play a role in SDF-1α/CXCL12 signaling and perhaps in the regulation of MAPK activity.

In summary, we have demonstrated that SDF-1α/CXCL12 action leading to Dok-1 activation is dependent on src kinases and on Pyk2. Several signaling pathways are induced by SDF-1α/CXCL12. These signaling pathways are regulated by positive and negative regulators. Dok-1 appears to play a negative role in SDF-1α/CXCL12 signaling and chemotaxis, and Pyk2 may play a positive role.

References

1. Bleul CC, Fuhlbrigge RC, Casasnovas JM, Aiuti A, Springer TA. A highly efficacious lymphocyte chemoattractant, stromal cell–derived factor 1 (SDF-1). J Exp Med. 1996;184:1101-1109.

2. Broxmeyer HE, Kim CH. Regulation of hemato-poiesis in a sea of chemokine family members with a plethora of redundant activities. Exp Hematol. 1999;27:1113-1123.

3. Bleul CC, Farzan M, Choe H, et al. The lympho-cyte chemoattractant SDF-1 is a ligand for LESTR/fusin and blocks HIV-1 entry. Nature. 1996;382:829-833.

4. Nagasawa T, Hirota S, Tachibana K, et al. Defects of B-cell lymphopoiesis and bone-marrow myelo-poiesis in mice lacking the CXC chemokine PBSF/SDF-1. Nature. 1996;382:635-638.

5. Zou YR, Kottmann AH, Kuroda M, Taniuchi I, Litt-man DR. Function of the chemokine receptor CXCR4 in haematopoiesis and in cerebellar de-velopment. Nature. 1998;393:595-599.

6. Ellis C, Moran M, McCormick F, Pawson T. Phos-phorylation of GAP and GAP-associated proteins by transforming and mitogenic tyrosine kinases. Nature. 1990;343:377-381.

7. Yamanashi Y, Baltimore D. Identification of the Abl- and rasGAP-associated 62 kDa protein as a docking protein, Dok. Cell. 1997;88:205-211.

8. Kaplan DR, Morrison DK, Wong G, McCormick F, Williams LT. PDGF beta-receptor stimulates ty-rosine phosphorylation of GAP and association of GAP with a signaling complex. Cell. 1990;61:125-133.

9. Hosomi Y, Shii K, Ogawa W, et al. Characteriza-tion of a 60-kilodalton substrate of the insulin re-ceptor kinase. J Biol Chem. 1994;269:11498-11502.

10. Yamanashi Y, Tamura T, Kanamori T, et al. Role of the rasGAP-associated docking protein p62(dok) in negative regulation of B cell receptor-mediated signaling. Genes Dev. 2000;14:11-16.

11. Boguski MS, McCormick F. Proteins regulating Ras and its relatives. Nature. 1993;366:643-654.

12. Lev S, Moreno H, Martinez R, et al. Protein ty-rosine kinase PYK2 involved in Ca(2+)-induced regulation of ion channel and MAP kinase func-tions. Nature. 1995;376:737-745.

13. Scheffzek K, Ahmadian MR, Wittinghofer A. GT-Pase-activating proteins: helping hands to complement an active site. Trends Biochem Sci. 1998;23:257-262.

14. Sasaki H, Nagura K, Ishino M, Tobioka H, Kotani K, Sasaki T. Cloning and characterization of cell adhesion kinase beta, a novel protein-tyrosine kinase of the focal adhesion kinase subfamily. J Biol Chem. 1995;270:21206-21219.

15. Avraham S, London R, Fu Y, et al. Identification and characterization of a novel related adhesion focal tyrosine kinase (RAFTK) from megakaryo-cytes and brain. J Biol Chem. 1995;270:27742-27751.

16. Yu H, Li X, Marchetto GS, et al. Activation of a novel calcium-dependent protein-tyrosine kinase: correlation with c-Jun N-terminal kinase but not mitogen-activated protein kinase activation. J Biol Chem. 1996;271:29993-29998.

17. Wange RL, Samelson LE. Complex complexes: signaling at the TCR. Immunity. 1996;5:197-205.

18. Valitutti S, Dessing M, Aktories K, Gallati H, Lan-zavecchia A. Sustained signaling leading to T cell activation results from prolonged T cell receptor occupancy: role of T cell actin cytoskeleton. J Exp Med. 1995;181:577-584.

19. Di Cristofano A, Niki M, Zhao M, et al. p62(dok), a negative regulator of Ras and mitogen-activated protein kinase (MAPK) activity, opposes leukemo-genesis by p210(bcr-abl). J Exp Med. 2001;194: 274-284.

20. Kim CH, Broxmeyer HE. In vitro behavior of he-matopoietic progenitor cells under the influence of chemoattractants: stromal cell–derived fac-tor-1, steel factor, and the bone marrow environ-ment. Blood. 1998;91:100-110.

21. Nemorin JG, Duplay P. Evidence that Lck-medi-ated phosphorylation of p56dok and p62dok may play a role in CD2 signaling. J Biol Chem. 2000; 275:14590-14597.

22. Lehmann JM, Riethmuller G, Johnson JP. Nck, a melanoma cDNA encoding a cytoplasmic protein consisting of the src homology units SH2 and SH3 [abstract]. Nucleic Acids Res. 1990;18:1048.

23. Mayer BJ, Hamaguchi M, Hanafusa H. A novel viral oncogene with structural similarity to phos-pholipase C. Nature. 1988;332:272-275.

24. Tsuchie H, Chang CH, Yoshida M, Vogt PK. A newly isolated avian sarcoma virus, ASV-1, car-ries the crk oncogene. Oncogene. 1989;4:1281-1284.

25. Boussiotis VA, Freeman GJ, Berezovskaya A, Barber DL, Nadler LM. Maintenance of human T cell anergy: blocking of IL-2 gene transcription by activated Rap1. Science. 1997;278:124-128.

26. Reedquist KA, Bos JL. Costimulation through CD28 suppresses T cell receptor-dependent acti-vation of the Ras-like small GTPase Rap1 in hu-man T lymphocytes. J Biol Chem. 1998;273: 4944-4949.

27. Holland SJ, Gale NW, Gish GD, et al. Juxtamem-brane tyrosine residues couple the Eph family

receptor EphB2/Nuk to specific SH2 domain proteins in neuronal cells. EMBO J. 1997;16:3877-3888.

28. Songyang Z, Shoelson SE, Chaudhuri M, et al. SH2 domains recognize specific phosphopeptide sequences. Cell. 1993;72:767-778.

29. Okabe S, Fukuda S, Broxmeyer HE. Src kinase, but not the src kinase family member p56lck, mediates stromal cell–derived factor 1α/CXCL12 induced chemotaxis of a T cell line. J Hematother Stem Cell Res. 2002;11:932-938.

30. Veillette A, Bookman MA, Horak EM, Bolen JB. The CD4 and CD8 T cell surface antigens are associated with the internal membrane tyrosine-protein kinase p56lck. Cell. 1988;55:301-308.

31. Carmo AM, Mason DW, Beyers AD. Physical association of the cytoplasmic domain of CD2 with the tyrosine kinases p56lck and p59fyn. Eur J Immunol. 1993;23:2196-2201.

32. Bustelo XR. Regulatory and signaling properties of the Vav family. Mol Cell Biol. 2000;20:1461-1477.

33. Arpaia E, Shahar M, Dadi H, Cohen A, Roifman CM. Defective T cell receptor signaling and CD8+ thymic selection in humans lacking zap-70 kinase. Cell. 1994;76:947-958.

34. Zhang XF, Wang JF, Matczak E, Proper JA, Groopman JE. Janus kinase 2 is involved in stromal cell–derived factor-1α–induced tyrosine phosphorylation of focal adhesion proteins and migration of hematopoietic progenitor cells. Blood. 2001;97: 3342-3348.

35. Lupher ML Jr, Reedquist KA, Miyake S, Langdon WY, Band H. A novel phosphotyrosine-binding domain in the N-terminal transforming region of Cbl interacts directly and selectively with ZAP-70 in T cells. J Biol Chem. 1996;271:24063-24068.

36. Wang JF, Park IW, Groopman JE. Stromal cell–derived factor-1α stimulates tyrosine phosphorylation of multiple focal adhesion proteins and induces migration of hematopoietic progenitor cells: roles of phosphoinositide-3 kinase and protein kinase C. Blood. 2000;95:2505-2513.

37. Okabe S, Fukuda S, Broxmeyer HE. Activation of Wiskott-Aldrich syndrome protein and its association with other proteins by stromal cell–derived factor-1α is associated with cell migration in a T-lymphocyte line. Exp Hematol. 2002;30:761-766.

A G-quadruplex-interactive agent, telomestatin (SOT-095), induces telomere shortening with apoptosis and enhances chemosensitivity in acute myeloid leukemia

M. SUMI[1], T. TAUCHI[1], G. SASHIDA[1], A. NAKAJIMA[1], A. GOTOH[1], K. SHIN-YA[3],
J.H. OHYASHIKI[2] and K. OHYASHIKI[1]

[1]First Department of Internal Medicine, [2]Intractable Immune-Disease Research Center, Tokyo Medical University,
Shinjuku-ku, Tokyo 160-0023; [3]Institute of Molecular and Cellular Biosciences,
The University of Tokyo, Bunkyo-ku, Tokyo 113-0032, Japan

Abstract. Telomerase, the ribonucleoprotein enzyme maintaining the telomeres of eukaryotic chromosomes, is up-regulated in the vast majority of human neoplasias but not in normal somatic tissues. Therefore, the telomerase complex represents a promising universal therapeutic target in cancer. Telomeric G-rich single-stranded DNA can adopt *in vitro* an intramolecular quadruplex structure, which has been shown to inhibit telomerase activity. We examined G-quadruplex interactive agent, telomestatin (SOT-095), for its ability to inhibit the proliferation of human leukemia cells, including freshly obtained leukemia cells. Telomere length was determined by either the terminal restriction fragment method or flow-FISH, and apoptosis was assessed by flow cytometry. Moreover, chemosensitivity was examined in telomestatin-treated U937 cells before ultimate telomere shortening. Treatment with telomestatin reproducibly inhibited telo-merase activity in U937 and NB4 cells followed by telomere shortening. Enhanced chemosensitivity toward daunorubicin and cytosine-arabinoside was observed in telomestatin-treated U937 cells, before ultimate telomere shortening. Telomere shortening associated with apoptosis by telomestatin was evident in some freshly obtained leukemia cells from acute myeloid leukemia patients, regardless of sub-types of AML and post-myelodysplasia AML. These results suggest that disruption of telomere maintenance by telomestatin limits the cellular lifespan of AML cells, as well. However, in a minority of AML patients apoptosis was not evident, thus indicating that resistant mechanism might exist in some freshly obtained AML cells. Therefore, further investigation of telomestatin as a therapeutic agent is warranted.

Correspondence to: Dr Tetsuzo Tauchi, First Department of Internal Medicine, Tokyo Medical University, 6-7-1 Nishishinjuku, Shinjuku-ku, Tokyo 160-0023, Japan
E-mail: ohyashik@tokyo-med.ac.jprr.iij4u.or.jp

Introduction

The reactivation of telomerase activity in most cancer cells supports the concept that telomerase is a relevant target in oncology, and telomerase inhibitors have been proposed as new potential anticancer agents (1,2). Several genetic experiments using a dominant-negative form of human telo-merase have demonstrated that telomerase inhibition can result in telomere shortening followed by proliferation arrest and cell death by apoptosis (3-5). One effective strategy for the design of telomerase inhibitors targets telomerase indirectly, via the telomeric substrate, and aims to block the interaction between the enzyme and the telomere (1). At the extreme 3'-termini of telomeres there are regions of single-stranded DNA, formed because of a limitation of the DNA poly-merization mechanism known as the end-replication problem (6,7). These regions have a G-rich, single-stranded structure assembled around a core stack of guanines arranged in almost-planar, hydrogen-bonded tetrads. Ionic conditions that favor quadruplex formation have been shown to inhibit telomerase (8), and small molecules that stabilize or promote the formation of quadruplexes also show inhibitory activity (9-12). Thus, quadruplex DNA presents a target of considerable importance in DNA-directed drug design.

Telomestatin (SOT-095) is a natural product isolated from *Streptomyces anulatus* 3533-SV4 and has been shown to stabilize G-quadruplex structures (13). The structural similarity between telomestatin and the G-quadruplex suggests that telomere disruption may be caused by the ability of telo-mestatin to either facilitate the formation of G-quadruplex structures or trap out G-quadruplexes that have already formed, thereby sequestering single-stranded d[T2AG3]n primer molecules (14). We have reported that telomestatin induced down-regulation of telomerase activity followed by ultimate telomere shortening and apoptosis in Philadelphia-positive leukemic cells (15). Moreover, it is demonstrated that telomestatin induced the activation of ATM and Chk2, and subsequently increased the expression of p21^{CIP1} and p27^{KIP1},
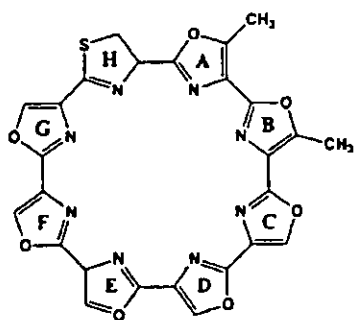
Figure 1. Structure of telomestatin. Telomestatin is a natural product isolated from *Streptomyses amulants* 3533-SV4. The structure of telomestatin is very similar to that of the G-tetrad.

indicating that telomere dysfunction induced by telomestatin activates the ATM-dependent DNA damage response (16). Therefore, telomestatin may effect acute myeloid leukemia,

including freshly obtained leukemia cells, and we assessed modulation of anti-leukemic agents that may induce DNA damage.

Materials and methods

Cells and agents. U937 cells and NB4 cells were obtained from the American Type Culture Collection (Rockville, MD). These cell lines were cultured in McCoy's 5A modified medium (Life Technology Inc.) supplemented with 10% fetal calf serum (Hyclone Laboratories, Logan, UT). Daunorubicin (DNR), cytosine arabinoside (Ara-C), etoposide (VP-16), vincristine (VCR), 6-mercaptopurine (6-MP), and methotrexate (MTX) were purchased from Sigma (St. Louis, MO). Telomestatin (SOT-095) has been described previously (Fig. 1), (13,14).

Telomerase assay and telomere measurement. Telomerase activity was measured by a telomere repeat amplification

Table I. Characteristics of acute myeloid leukemia cells treated with telomestatin *in vitro*.

UPN	Age/ gender	Diagnosis	WBC	Blast (%)	Karyotypes	Surface markers (CD)	Source of in vitro study	Percentage of APO 2.7		Telomere length (kb)	
								Before	After	Before	After
1	54/F	AML-M1-relapse	9,000	31	46,XX	13/33/117/34/71/DR/7	PB	1.58	28.30	9.3	6.1
2	59/M	AML-M1	16,100	75	33-39,XY,-10, -11,-12,-16,-17, -18,-19,-20	13/33	BM	4.19	21.70	5.7	5.3
3	61/M	AML-M2	24,600	97	46/XY/46/XY add(21)(q22)	13/33/117/ 34/56/DR/7	PB	4.26	76.70	ND	ND
4	52/M	AML-M3	20,100	16 (66)	46,XY,t(15;17) (q22;q21),46,XY, idem,add(7)(q31)	13/14/38/33	PB	18.20	28.80	19.8	16.7
5	47/M	AML-M4Eo	31,600	82	46,XY/45,X,-Y, inv(16)(p13q22)/ 46,X,-Y,idem,+21	13/33/34/ 117/DR	BM	12.10	17	8.9	5.9
6	53/M	Post-MDS AML	3,000	16	47,XY,-7,-18, +3mar	13/33/117/ 34/71/DR	BM	2.71	17.90	5.5	5.2
7	74/M	Post-MDS AML	6,800	48	46,XY	13/15/117/34/ 56/71/DR	BM	4.87	12.20	ND	ND
8	63/M	Post-MDS AML	9,600	83	46,XY	15/33/64/65/ 11b/56/DR	PB	10.20	62	13.5	5.8
9	70/M	Post-MDS AML	5,400	48	46,XY,der(7) t(1;7)(q10;p10)/47, XY,idem,+8/48, XY,idem,+8,+8	13/33/94/ 117/34/DR	BM	4.04	4.50	ND	ND

Gender: M, male; F, female. Source of *in vitro* study: PB, peripheral blood; BM, bone marrow. Telomere length: before, before telomestatin treatment; after, after telomestatin treatment.

protocol (TRAP) assay using a TRAPeze telomerase detection kit (Oncor, Gaithersburg, MD) (17,18). To measure terminal restriction fragment (TRF) length, genomic DNA was digested with restriction enzymes (HinfI or RsaI) and assessed using the Telo TTAGGG telomere length assay kit (Roche Molecular Biochemicals, Mannheim, Germany). Smears of the developed films were captured on an Image Master (Pharmacia Biotech, Uppsala, Sweden), and defined the TRF in each sample as the peak intensity of telomeric length, in kilobases (kb), by densitometry (19).

We employed flow-FISH, since this method is very useful for analysis of clinical samples with small numbers of cells. Telomere length measurements of primary leukemia cells were performed by flow-FISH, as previously described (21,22). Briefly, cells were washed in phosphate-buffered saline and were divided equally into two 1.5-ml tubes. After centrifugation cells were resuspended in the hybridization mixture (10^5 cells/μl) with 0.3 μg/ml telomere-specific FITC-conjugated PNA probe (Dako, Denmark). The cells were washed three times and resuspended in DNA-staining solution with propidium iodide and RNase A. The samples were then analyzed by flow cytometry (Epics XL Beckman Coulter, Fullerton, CA). Daily shifts in the linearity of the flow cyto-meter and fluctuations in the laser intensity and alignment were compensated for by using FITC-labeled fluorescent beads (Quantum-24 Premixed; Flow Cytometry Standards, San Juan, Puerto Rico). To analyze the day-to-day variation in flow-FISH results, aliquots of cells derived from a primary calf thymus cells were analyzed in each experiment. Formula: telomere length = 4.551+0.077 (AU/telomere fluorescence of referential calf thymus cell), AU = telomere fluorescence of sample with probe - telomere fluorescence of sample without probe.

Apoptosis assay. The incidence of apoptosis was determined by flow cytometric analysis with FITC-conjugated APO2.7 monoclonal antibody (clone 2.7), which was raised against the 38-kDa mitochondrial membrane protein (7A6 antigen) and is expressed by cells undergoing apoptosis (15).

Primary leukemic cells. Primary leukemic blasts were freshly isolated from 9 patients with acute myeloid leukemia after obtaining informed consent from patients who had been referred to the Tokyo Medical University Hospital. The nine leukemia patients consisted of two AML-M1, one AML-M2, one AML-M3, one AML-M4Eo, and four post-myelo-dysplastic AML (post-MDS AML) (Table I). Leukemic enriched fraction was obtained by Ficoll-Hypaque gradient method and analyzed for apoptosis test and telomere length was measured using the flow-FISH.

Statistical analysis. Comparisons between groups were analyzed by Student's t-test. Values of p<0.05 were considered to indicate statistical significance. Statistical tests were performed with the Microsoft Word Excel software package (Brain Power, Calabashes, CA) on a Macintosh personal computer.

Results

Effects of telomestatin on telomerase activity and telomere length in a human leukemia cell line. To study the effects of
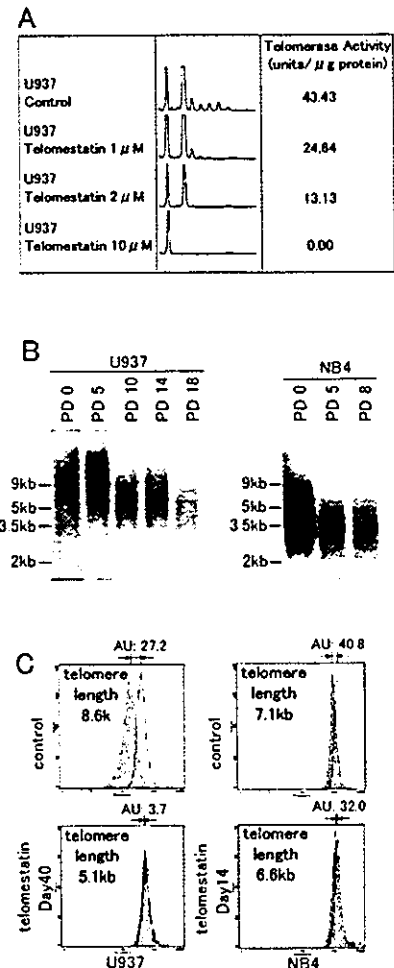

Figure 2. Effects of telomestatin on telomerase activity and telomere length in leukemia cells. (A), Effect of telomestatin on telomerase activity in U937 cells. U937 cells were incubated with the indicated concentrations of telo-mestatin for 48 h, then telomerase activity was examined by a TRAP assay. Telomerase activity was suppressed by telomestatin in a dose-dependent manner. (B), Telomere length in U937 cells and NB4 cells was assessed for telomere restriction fragment size by Southern blot analysis with a telomeric probe. In both myeloid leukemia cell lines, telomere length was progressively shortened after telomestatin treatment at indicated population doubling (PD). (C), U937 cells and NB4 cells were cultured with or without 2 μM of telomestatin for the number of days indicated, and telomere length was determined by flow-FISH analysis. This indicates, in combination with (B), that flow-FISH method is reproducible to determine telomere length in leukemia cells.

telomestatin on telomerase activity, we first cultured U937 cells with various concentrations of telomestatin for 48 h. Telomestatin appears to be a potent telomerase inhibitor, with 50% inhibition at ~2 μM (Fig. 2A). To examine the long-term effects of telomestatin on U937 cells and NB4 cells, it was necessary to identify the drug concentration window in which telomerase could be inhibited without extensive inhibition of cell proliferation. Addition of 2 μM of telomestatin had no effect on short-term cell viability or proliferation, as determined in a 7-day cytotoxicity assay. Therefore, we used 2 μM as the treatment concentration in long-term cultivation experiments.

In the presence of telomestatin, the TRF length of U937 cells shortened progressively from 9.5 to 5.0 kb at population
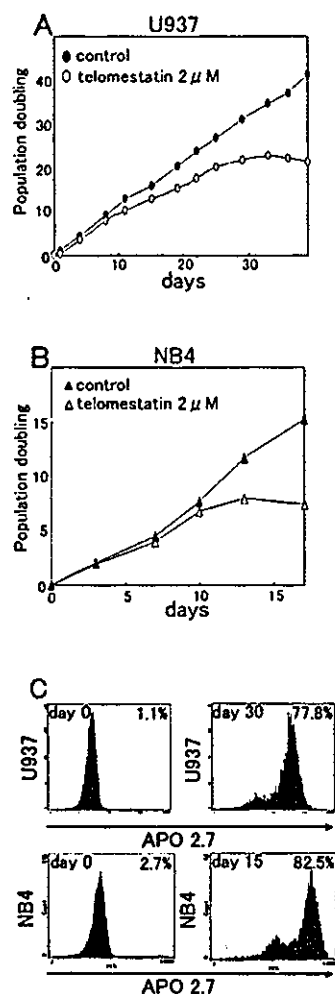
Figure 3. Effects of telomestatin on cell proliferation. U937 cells (A) and NB4 cells (B) were plated in 24-well plates in the presence of 2 μM of telomestatin in 0.1% methanol. Control cells were treated with 0.1% methanol. Cultures were replated every 3 or 4 days to maintain log-phase growth and to calculate the growth rate. (C), U937 cells and NB4 cells were cultured with 2 μM of telomestatin for the number of days indicated. The incidence of apoptosis was determined by flow cytometric analysis with FITC-conjugated APO 2.7 mAb (clone 2.7). Most leukemia cells showed apoptosis after incubation of telomestatin: 77.8% of telomestatin treated U937 cells at 30 day and 82.5% of telomestatin treated NB4 cells at 15 day showed apoptosis.
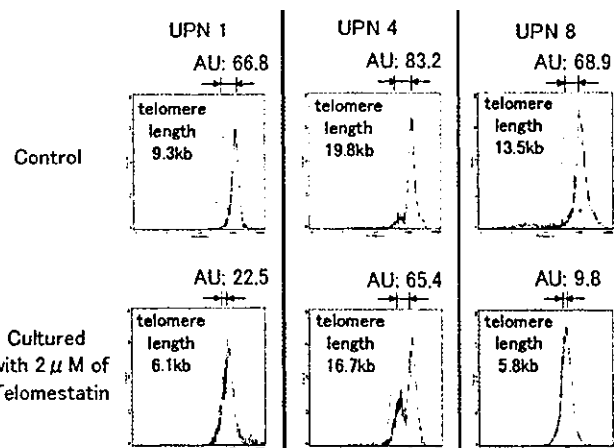

Figure 4. Effects of telomestatin on telomere reduction in freshly obtained human acute myeloid leukemia cells. Primary leukemia cells were incubated for 10 days in the absence or presence of 2 μM telomestatin. The telomere length was determined by flow-FISH. The telomere lengths were assessed using the formula (Materials and methods). Representative cases are shown.

with distinctive morphological features associated with apoptosis. The percentage of apoptosis increased in U937 cells from 1.1 to 77.8% at day 30 and in NB4 cells from 2.7 to 82.5% at day 15 (Fig. 3C). These results demonstrate that telomestatin inhibits telomerase activity in myeloid leukemia cells, resulting in telomere shortening, which may lead to subsequent induction of apoptosis.

Telomere shortening and induction of apoptosis in primary acute leukemia cells after exposure to telomestatin. Freshly isolated leukemic cells (>85% blast cells) were incubated in suspension cultures in the absence or presence of 2 μM of telomestatin for 10 days, and the occurrence of apoptosis was examined by APO2.7 antibody testing; in some case, telomere length was determined by flow-FISH, as well. Eight of 9 samples showed an increasing frequency of apoptosis after treatment of telomestatin, and 6 of them (UPN 1, 2, 3, 6, 7, and 8) showed more than two-holds increase in the percentage of apoptosis (Table I). Representatively, addition of 2 μM of telomestatin increased the incidence of apoptosis (from 1.58 to 28.3%), accompanied by telomere shortening (from 9.3 to 6.1 kb) in UPN 1. The same effect was also reproducible in UPN 8: apoptosis occurred (from 10.2 to 62.0%) accompanied by telomere shortening (from 13.5 to 5.8 kb) after 10 days incubation with telomestatin (Fig. 4). These results suggest that telomere shortening by telomestatin induces apoptosis in some primary blast cells from acute leukemia, regardless of sub-types of AML. This effect seemed not to be restricted in de novo AML but post-MDS AML.

However, the frequency of apoptosis was <20% in some cases (4/9 patients). One patient with post-MDS AML (UPN 9) did not show an increase in percentages of APO 2.7-positive cells after telomestatin treatment (from 4.04 to 4.5%). One possibility might be due to the timing of determination of apoptosis in this study. Another plausible explanation for limiting effect in inducing apoptosis might be due to alternative mechanism of telomere elongation (ALT) (22,23). Leukemic
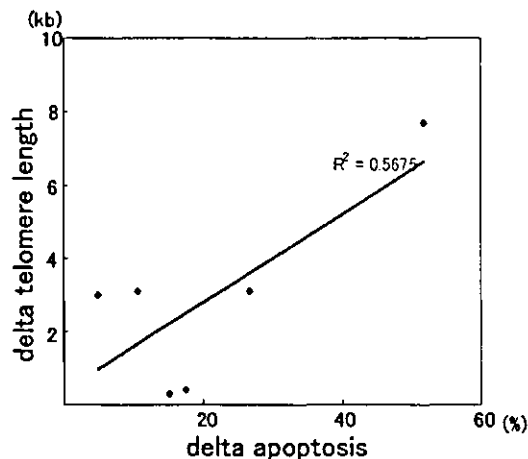
doubling (PD) 18, and TRF length in telomestatin-treated NB4 cells also shortened from 4.8 to 3.5 kb (Fig. 2B). The telomere shortening after cultivation of 2 μM telomestatin was also confirmed by flow-FISH analysis using the PNA probe (Fig. 2C). This clearly indicates that telomere length, as well as TRF length that includes sub-telomeric region, actually shortened at the time of appropriate PD in telomestatin-treated myeloid leukemia cells (U937 and NB4 lines).

Effects of telomestatin on cell proliferation and apoptosis. The growth kinetics of telomestatin-treated cells initially did not differ from those of untreated control cells, regardless of the cell line used. After 30 days (around PD 20), telomestatin-treated U937 cells showed an almost complete inhibition of proliferation (Fig. 3A), whereas telomestatin-treated NB4 cells ceased to proliferate after 13 days (around PD 8) (Fig. 3B)

Figure 5. Correlation between delta-telomere and delta-apoptosis in freshly obtained acute myeloid leukemia cells with 10-days culture of 2 μM telomestatin. Vertical axis shows delta-telomere length = telomere length with telomestatin-telomere length without telomestatin (kb). Horizontal axis shows delta-apoptosis = apoptosis with telomestatin-apoptosis without telomestatin (%).

Figure 6. Enhancement of apoptosis from DNR or AraC treatment in telomestatin-treated U937 cells. U937 cells cultured with 2 μM telomestatin at PD 10 were incubated with the indicated concentrations of DNR (A) or AraC (B) for 48h. The incidence of apoptosis was determined by flow cytometric analysis with APO 2.7 mAb. Similar results were obtained in two independent experiments.

cells from UPN 4 did not show remarkable shortening of telomere length after telomestatin treatment (from 19.8 to 16.7 kb) with a limited effect for apoptosis (from 18.2 to 28.8%) (Fig. 4). Though there seems to be variety between telomere reduction and the frequency of apoptosis after telomestatin treatment *in vitro* in leukemia cells obtained from AML patients, there was a correlation between reduction of the length of telomeres and the frequency of apoptosis (Fig. 5). This indicates that apoptosis in AML cells by telomestatin might be related to the reduction of telomere length.

Enhanced apoptosis in response to chemotherapeutic agents in telomestatin-treated U937 cells. We next assessed the effects of telomerase inhibition in modulating responses to chemotherapeutic agents at relatively early-passage telomestatin-treated U937 cells (PD10), since early-passage telomestatin-treated U937 cells showed partial induction of apoptosis (<10%) and limited cessation of cellular proliferation (Fig. 3A), without telomerase activity. Subsequently, the telomestatin-treated U937 cells were incubated with the chemotherapeutic agents for 48 h. The U937 cells without pre-treatment with telomestatin showed approximately 11% apoptosis after 50 nM DNR treatment, while 49% telomestatin treated cells showed apoptosis after the same concentration of DNR (11.4±6.4% vs. 48.9±12.3%; p=0.04). This tendency was also evident after 500 nM Ara-C treatment (20.7±1.6% vs. 48.8±8.4%; p=0.027). The lower concentrations of DNR (10 nM) or Ara-C (100 nM) treated U937 cells showed an enhanced induction of apoptosis as well, but not significant (p=0.315 and p=0.113, respectively) (Fig. 6). By contrast, enhanced chemosensitivity was not observed in cells exposed to VCR, VP-16, 6-MP, or MTX (data not shown). This enhanced sensitivity regarding apoptosis to some classes of chemotherapeutic agents indicates that there is cytotoxic synergy between telomere dysfunction and these agents.
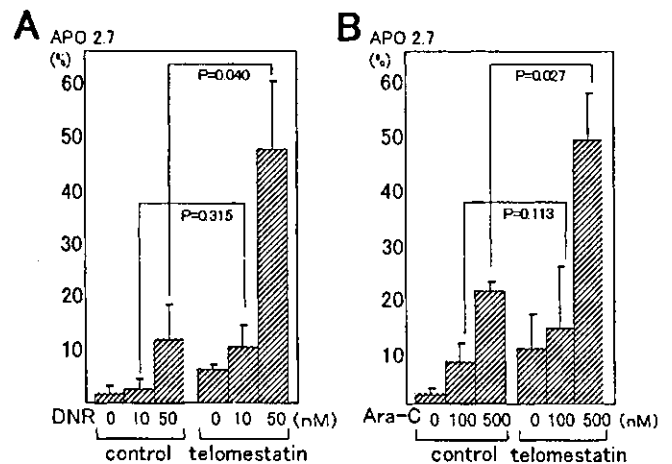
Discussion

Telomere shortening is thought to be important in the regulation of cellular senescence and up-regulation of telomerase activity may be critical in the development of neoplastic cells. One prediction of this model is that specific inhibition for telomerase function alters the growth properties relating to telomere dysfunction of neoplastic cells and thus may be candidates of a new strategy for universal anti-neoplastic therapy (1). Genetic experiments using a dominant-negative form of human telomerase demonstrated that telomerase inhibition can result in telomere shortening followed by proliferation arrest and cell death by apoptosis (3-5). Several other strategies to inhibit telomerase activity have been reported so far: a recent study described N3'>P5' thio-phosphoramidate oligonucleotides as telomerase template antagonists (GRN163), which should display improved clinical efficacy (25). These approaches selectively act on neoplastic cells with high telomerase activity and are suitable for 'target therapy' for neoplasia. However, this method limits the proportion of the completely telomerase-negative clone that sometimes exists in telomerase-positive population or tumors with telomerase-independent telomere elongation (22,23). Moreover, telomerase activity in human acute leukemia is generally not high when compared to solid tumors (26,28), thus indicating that target therapy against telomerase in human acute leukemia might be limited to monotherapy.

In the current study, we tested the therapeutic possibility of telomestatin for acute myeloid leukemia. Telomestatin induces telomere shortening, as well as down-regulation of telomerase activity, and apoptosis in human myeloid leukemia cell lines. Since telomestatin selectively stabilizes intramolecular G-quadruplexes, including telomere sequences [T_2AG_3], telomestatin might also exert an effect directly and is expected to induce more rapid onset of telomere shortening and cellular senescence. Since effectiveness of target therapy against the telomerase actually depends on the 'end-

replication problem', cells in the arrest phase may escape from the attack. Moreover, action of telomestatin may be independent of the levels of telomerase activity, thus human acute leukemia might be suitable for target therapy with telomestatin. We also observed that telomere shortening by telomestatin also induced apoptosis in some primary blast cells freshly obtained from AML patients. However, some fresh AML cells with shortened telomeres exceptionally showed limited effect in inducing apoptosis after telomestatin treatment. It should be clarified whether the determination timing of apoptosis in this study is enough to detect cellular senescence or the existence of abolish mechanism of telomestatin. Although we did not have a chance to measure telomerase activity in fresh AML cells in this study, telomestatin might affect growth and survival of acute leukemia cells with or without high levels of telomerase activity.

G-quadruplex-forming sequences are also found in several transcriptional regulatory regions of important oncogenes, including c-myc, c-myb, c-fos, and c-abl (29). Because of the polypurine-polypyrimidine nature of these duplex sequences, which contain 4 or more runs of clusters of three or more guanines on the purine-rich strand, they often show a single-stranded character and hence are hypersensitive to nucleases. In the c-myc promoter, the purine- and pyrimidine-rich strands bind transcription factors [cellular nucleic-acid-binding protein (CNBP), and heterogeneous nuclear ribonuclear protein (hnRNP)] that are required for transcriptional activation (30). As these elements can also form G-quadruplex and I-motif structures, it is possible that the secondary DNA structures inactivate transcription, and their conversion to duplex regions is required for transcriptional activation (31). These issues indicate possible benefit to use telomestatin not only for the purpose of telomere-telomerase inhibitor but also transcriptional inhibitor of key gene(s) for proliferation of leukemic cells.

Our study using fresh AML cells demonstrated that reduction of telomere varied from 0.3 to 7.8 kb after only 10 days of culture with telomestatin. It is too early to induce telomere shortening only due to the 'end-replication problem' after shutting off telomerase activity. Telomere reduction usually takes place 100 bp around one cell cycle and 4-5 cell cycles during a 10 day-culture, thus several kb reductions of telomeres in our experiments using freshly obtained AML cells might be due to telomere-disruption mechanism by telomestatin. This supports the concept that telomestatin directly attacks telomeres and induces telomere shortening, resulting in apoptosis of acute leukemia cells. Thus, telomestatin might have multi-function for not only a telomerase-telomere maintenance mechanism but also regulation mechanism of certain oncogene(s).

Telomerase-specific inhibitors usually show certain lag-time to cellular senescence until telomere shortening. Therefore, we assessed chemosensitivity before ultimate telomere shortening in acute myeloid leukemia cells, and confirmed that DNR and Ara-C could be beneficial in combination with telomestatin in inducing cell death. Lee et al reported that neoplastic cells from telomerase RNA null mice (mTERC-/-) showed enhanced chemosensitivity to DNR or related double-strand DNA break (DSB)-inducing agents (32). Telomere dysfunction, rather than telomerase inhibition,

is proposed to be the principal determinant governing chemosensitivity specifically to DSB-inducing agents (32). We also reported that telomestatin induced the activation of ATM and Chk2, and subsequently increased the expression of $p21^{CIP1}$ and $p27^{KIP1}$, indicating that telomere dysfunction induced by telomestatin activates the ATM-dependent DNA damage response (16). However, we were unable to detect enhanced induction of apoptosis by VP-16, VCR, 6-MP, or MTX in telomestatin-treated U937 cells. VP-16 is a topo-isomerase II inhibitor and induces DSBs, as does DNR. Therefore, it will be important to resolve the question of why these two different kinds of DSB-inducing agent have different effects on chemosensitivity in telomestatin-treated cells. Although the exact mechanism of the enhanced induction of apoptosis in telomestatin-treated cells requires further elucidation, telomerase inhibition and telomere dysfunction has previously been shown to enhance the chemosensitivity of tumor cells to DNA-damaging agents (33).

References

1. Bearss DJ, Hurley LH and Von Hoff DD: Telomere maintenance mechanisms as a target for drug development. Oncogene 19: 6632-6641, 2000.
2. White LK, Wright WE and Shay JW: Telomerase inhibitors. Trends Biotech 19: 114-120, 2001.
3. Hahn WC, Stewart SA, Brooks MW, York SG, Eaton E, Kurachi A, Beijersbergen RL, Knoll JHM, Meyerson M and Weinberg RA: Inhibition of telomerase limits the growth of human cancer cells. Nat Med 5: 1164-1170, 1999.
4. Zhang X, Mar V, Zhou W, Harrington L and Robinson MO: Telomere shortening and apoptosis in telomerase-inhibited human tumor cells. Genes Dev 13: 2388-2399, 1999.
5. Tauchi T, Nakajima A, Sashida G, Shimamoto T, Ohyashiki JH, Abe K, Yamamoto K and Ohyashiki K: Inhibition of human telomerase enhances the effect of the tyrosine kinase inhibitor, imatinib, in BCR-ABL-positive leukemia cells. Clin Cancer Res 8: 3341-3347, 2002.
6. Watson JD: Origin of concatameric T7 DNA. Nature 239: 197-201, 1972.
7. Olovnikov AM: A theory of marginotomy. J Ther Biol 41: 181-190, 1973.
8. Zahler AM, Williamson JR, Cech TR and Prescott DM: Inhibition of telomerase by G-quartet DNA structures. Nature 350: 718-720, 1991.
9. Sun D, Thompson B, Cathers BE, Salazar M, Kerwin SM, Trent JO, Jenkins TC, Neidle S and Hurley LH: Inhibition of human telomerase by a G-quadruplex-interactive compound. J Med Chem 40: 2113-2116, 1997.
10. Wheelhouse RT, Sun D, Han H, Han FX and Hurley LH: Cationic porphyrins as telomerase inhibitors: interaction of tetra (N-methyl-4-pyridyl) porphyrin with quadruplex DNA. J Am Chem Soc 120: 3261-3262, 1998.
11. Perry PJ and Jenkins TC: Recent advances in the development of telomerase inhibitors for the treatment of cancer. Exp Opin Invest Drugs 8: 1981-2008, 1999.
12. Izbicka E, Wheelhouse RT, Raymond E, Davidson KK, Lawrence RA, Sun D, Windle BE and Hurley LH: Effects of cationic porphyrins as G-quadruplex interactive agents in human tumor cells. Cancer Res 59: 639-644, 1999.
13. Shin-ya K, Wierzba K, Matsuo K, Ohtani T, Yamada Y, Furihata K, Hayakawa Y and Seto H: Telomestatin, a novel telomerase inhibitor from Streptomyces anulatus. J Am Chem Soc 123: 1262-126, 2001.

14. Kim MY, Vankayalapati H, Shin-Ya K, Wierzba K and Hurley LH: Telomestatin, a potent telomerase inhibitor that interacts quite specifically with the human telomeric intra-molecular G-quadruplex. J Am Chem Soc 124: 2098-2099, 2002.

15. Nakajima A, Tauchi T, Sashida G, Sumi M, Abe K, Yamamoto K, Ohyashiki JH and Ohyashiki K: Telomerase inhibition enhannces apoptosis in human acute leukemia cells: possibility of anti-telomerase therapy. Leukemia 17: 560-567, 2003.

16. Tauchi T, Shin-ya K, Sashida G, Sumi M, Nakajima A, Simamoto T, Ohyashiki JH and Ohyashiki K: Activity of novel G-quadruplex-interactive telomerase inhibitor, telomestatin (SOT-095), against human leukemia cells: involvement of ATM-dependent DNA damage response pathways. Oncogene 14: 5338-5347, 2003.

17. Piatyszeck MA, Kim MY, Weinrich SL, Hiyama K, Hiyama E, Wright WE and Shay JW: Detection of telomerase activity in human cells and tumors by a telomeric repeat amplification protocol (TRAP). Method Cell Sci 17: 1-15, 1995.

18. Ohyashiki JH, Ohyashiki K, Toyama K and Shay JW: A non-radioactive, fluorescence-based telomeric repeat amplification protocol to detect and quantitate telomerase activity. Trends Genet 12: 395-396, 1996.

19. Iwama H, Ohyashiki K, Ohyashiki JH, Hayashi S, Yahata N, Ando K, Toyama K, Hoshika A, Takasaki M, Mori M and Shay JW: Telomeric length and telomerase activity vary with age in peripheral blood cells obtained from normal individuals. Hum Genet 102: 397-402, 1998.

20. Rufer N, Brummendorf TH, Kolvraa S, Bischoff C, Christensen K, Wadsworth L, Schulzer M and Lansdorp PM: Telomere fluorescence measurements in granulocytes and T lymphocyte subsets point to a high turnover of hematopoietic stem cells and memory T cells in early childhood. J Exp Med: 157-167, 1999.

21. Misawa M, Tauchi T, Sashida G, Nakajima A, Abe K, Ohyashiki JH and Ohyashiki K: Inhibition of human telomerase enhances the effect of chemotherapeutic agents in lung cancer cells. Int J Oncol 21: 1087-1092, 2002.

22. Bryan TM, Englezou A, Gupta J, Bacchetti S and Reddel RR: Telomere elongation in immortal human cells without detectable telomerase activity. EMBO J 14: 4240-4248, 1995.

23. Dunham MA, Neumann AA, Fasching CL and Reddel RR: Telomere maintenance by recombination in human cells. Nat Genet 26: 447-450, 2001.

24. Delhommeau F, Thierry A, Feneux D, Lauret E, Leclercq E, Coutier MH, Stainteny F and Vainchenker W: Telomere dysfunction and telomerase reactivation in human leukemia cell lines after telomerase inhibition by the expression of a dominant-negative hTERT mutant. Oncogene 21: 8262-8271, 2002.

25. Asai A, Oshima Y, Yamamoto Y, Uochi T, Kusakawa H, Akinaga S, Yamashita Y, Pongracz K, Pruzan R, Wunder E, Piatyszek M, Li S, Chin AC, Harley CB and Gryaznov S: A novel telomerase template antagonist (GRN163) as a potential anticancer agent. Cancer Res 63: 3931-3939, 2003.

26. Ohyashiki JH, Ohyashiki K, Iwama H, Hayashi S, Toyama K and Shay JW: Clinical implications telomerase activity levels in acute leukemia. Clin Cancer Res 3: 619-624, 1997.

27. Engelhardt M, MacKenzie K, Drullinsky P, Silver RT and Moore MA: Telomerase activity and telomere length in acute and chronic leukemia, pre- and post-ex vivo culture. Cancer Res 60: 610-617, 2000.

28. Ohyashiki JH, Sashida G, Tauchi T and Ohyashiki K: Telomeres and telomerase in hematopoietic neoplasia. Oncogene 21: 680-687, 2002.

29. Hurley LH: DNA and its associated processes as targets for cancer therapy. Nat Rev Cancer 2: 188-200, 2002.

30. Simonsson T, Pecinka P and Kubista M: DNA tetraplex formation in the control region of c-myc. Nucleic Acids Res 26: 1167-1172, 1998.

31. Siddiqui-Jain A, Grand CL, Bearss DJ and Hurley LH: Direct evidence for a G-quadruplex in a promoter region and its targeting with a small molecule to repress c-MYC transcription. Proc Natl Acad Sci USA 99: 11593-11598, 2002.

32. Lee KH, Rudolph KL, Ju YJ, Greenberg RA, Cannizzaro L, Chin L, Weiler SR and DePinho RA: Telomere dysfunction alters the chemotherapeutic profile of transformed cells. Proc Natl Acad Sci USA 98: 3381-3386, 2001.

33. Stewart SA, Hahn WC, O'Connor BF, Banner EN, Lundberg AS, Modha P, Mizuno H, Brooks MW, Fleming M, Ziomonjic DB, Popescu NC and Weinberg RA: Telomerase contributes to tumorigenesis by a telomere length-independent mechanism. Proc Natl Acad Sci USA 99: 12606-12611, 2002.

ELSEVIER

Leukemia Research

www.elsevier.com/locate/leukres

Letter to the Editor

Successful treatment with imatinib mesylate of hypereosinophilic syndrome (chronic eosinophilic leukemia) with myelofibrosis

1. To the Editor

Imatinib mesylate (imatinib, STI571, Glivec; Novartis Pharmaceuticals, Basel, Switzerland) is a potent and selective inhibitor of the tyrosine kinase activity of *BCR-ABL*, c-kit (CD117), and platelet-derived growth factor receptor (PDGFR) [1]. Imatinib is now widely used for Philadelphia-positive leukemia as a target therapy, and is also effective for patients with chronic myeloproliferative disorders with t(5;12)(q33;q13) that results in fusion of *ETV6-PDGFR*-β [2]. Although its exact mechanism of action is unknown, imatinib is currently reported to be effective for some patients with hypereosinophilic syndrome (HES) [3–6]. Here we report another patient with HES/chronic eosinophilic leukemia (CEL) with myelofibrosis who responded to imatinib.

The patient was a 41-year-old male first diagnosed with HES and myelofibrosis in March 1997, based on marrow biopsy and bronchoalveolar lavage (32% eosinophils). He was treated with prednisolone, interferon-α, hydroxyurea, and cyclosporin A without significant efficacy for his eosinophilia and complained of asthma-like respiratory symptoms. He was treated with prednisolone (10 mg), hydroxyurea (1500 mg), and cyclosporin A (150 mg) until July 2002, but his eosinophilia ($>6 \times 10^9\,l^{-1}$) persisted. Although cytogenetic study at the time of diagnosis revealed a normal male karyotype, chromosome study using peripheral blood in March 2002, disclosed a clonal abnormality (46,XY,ins(1)(q21?) [19 cells]/46,XY [3 cells]), indicating disease progression to CEL [7]. Fluorescence in situ hybridization (FISH) analysis of BCR-ABL fusion revealed 0% positive (0/108 cells).

After obtaining written informed consent from the patient, imatinib (100 mg per day, p.o. based on the previous report [3]) was started on 30 July 2002. Before administration of imatinib, his white blood cell count (WBC) was $10 \times 10^9\,l^{-1}$, including 62.5% eosinophils (Eo; absolute count $6250 \times 10^6\,l^{-1}$), a hemoglobin (Hb) of 90 g/l, and a platelet (Plt) count of $132 \times 10^9\,l^{-1}$. At the time of admission, he had anemic conjunctiva and hepatosplenomegaly (liver 7 cm and spleen 7 cm palpable), Biochemical data were all within the normal range, including IgE level, except for elevation of LDH. The serum level of interleukin (IL)-5

was 38 pg/ml (detectable limit <5 pg/ml) (Fig. 1). Before administration of imatinib, hydroxyurea and cyclosporin A were discontinued for 3 days. On the seventh day of imatinib administration, absolute eosinophil fell to within the normal range (4%, absolute count $112 \times 10^6\,l^{-1}$), and asthma-like respiratory symptoms disappeared completely. Imatinib (100 mg per day, p.o.) was administered for 7 days, and then maintained (100 mg per day, twice a week). Until the end of October 2002, no eosinophilia was noted (<5%), and there were no notable adverse effects. Currently, his liver is not palpable, but his spleen is still palpable 5 cm below the left costal margin, with improvement of anemia (hemoglobin: 144 g/l). After administration of imatinib (20th day), levels of serum IL-5 and serum fibroblast growth factor (FGF)-basic became undetectable, but no notable changes in the elevated levels of transforming growth factor-beta1 (TGF-β1), vascular endothelial growth factor (VEGF), and PDGF-AB were noted before to after administration (Fig. 1).

Gleich et al. reported that of five HES patients, four responded to imatinib, all of whom were male with a normal karyotype [3]. Although they concluded that undetectable levels of IL-5 might predict the efficacy of imatinib [3], they thereafter described that all four responding patients of seven HES/eosinophilia-associated chronic myeloid disorder had elevated serum IL-5 levels [6]. It was suggested that c-kit might not be a target for imatinib mesylate in their HES patients, since the patients had no loop mutation (D816V) of c-kit [3]. Ault et al. reported a 54-year-old HES patient who responded to imatinib whose eosinophils expressed stem cell factor; the authors speculated an effect against PDGFR in the mechanism of efficacy of imatinib for HES [4]. Pardanani et al. screened exons encoding the intracellular catalytic domains and extracellular ligand binding domains of PDGFRβ and c-kit, demonstrating only previously known polymorphisms [6]. Recently Cools et al. reported a novel fusion tyrosine kinase-FIP1L1-PDGFRA might be a therapeutic target of imatinib for HES [8].

In the present case, IL-5 became undetectable after treatment with imatinib. No notable change was observed in the level of PDGF before to after imatinib therapy. It should be clarified that the blockage of signal transduction of PDGFR by imatinib might aid dramatic reduction of eosinophils in vivo. The clinical implications of elevated PDGF are not easily evaluable [9], since our patient had myelofibrosis as well. Level of FGF decreased after imatinib therapy, and this may be related to the myelofibrosis in our patient. Although the exact mechanism of efficacy of imatinib for HES
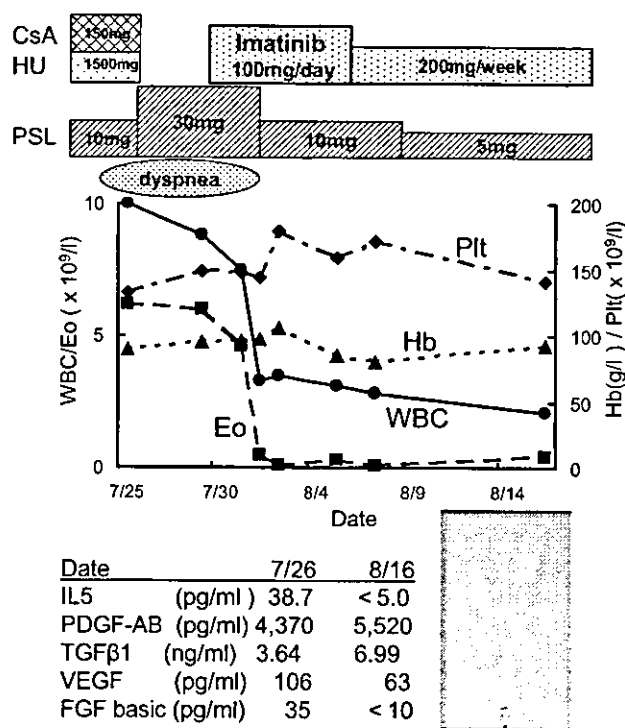
Fig. 1. Clinical course and hematologic findings during imatinib treatment for chronic eosinophilic leukemia. The elevated levels of serum interleukin-5 (38.7 pg/ml: detectable limit <5.0 pg/ml) and fibroblast growth factor-basic (35 pg/ml: detectable limit <10 pg/ml) became undetectable after imatinib therapy, whereas no notable changes were detectable in levels of PDGF-AB (normal range, 474–2975 pg/ml), TGF-β1 (normal range, 1.56–3.24 ng/ml), or VEGF (normal range, 62–707 pg/ml) before to after imatinib treatment. The insert shows ins(1)(q21;?) abnormality in this case.

is still unknown, imatinib might be a powerful agent for the treatment of HES patients, including those with cells of a neoplastic nature, i.e. CEL.

Acknowledgements

References

[1] Heinrich MC, Griffith DJ, Druker BJ, Wait CL, Ott KA, Zigler AJ. Inhibition of c-kit receptor tyrosine kinase activity by STI 571* a selective tyrosine kinase inhibitor. Blood 2000;96:925–32.

[2] Apperley JF, Gardembas M, Melo JV, Russell-Jones R, Bain BJ, Baxter EJ, et al. Response to imatinib mesylate in patients with chronic myeloproliferative diseases with rearrangements of the platelet-derived growth factor receptor beta. New Engl J Med 2002;347:481–7.

[3] Gleich GJ, Leiferman KM, Pardanani A, Tefferi A, Butterfield JH. Treatment of hypereosinophilic syndrome. Lancet 2002;359:1577–8.

[4] Ault P, Cortes J, Koller C, Kaled ES, Kantarjian H. Response of idiopathic hypereosinophilic syndrome to treatment with imatinib mesylate. Leuk Res 2002;26:881–4.

[5] Schaller JL, Burkland GA. Case report: rapid and complete control of idiopathic hypereosinophilia with imatinib mesylate. Med Gen Med 2001;3:9.

[6] Pardanani AD, Reeder TL, Porrata LF, Li CY, Tazelaar HD, Baxter EJ, et al. Imatinib therapy for hypereosinophilic syndrome and other eosinophilic disorders. Blood 2003;101:3391–7.

[7] World Health Organization classification of tumors. Pathology and genetics, tumor of haematopoietic and lymphoid tissues. Jaffe WRC Press; 2001.

[8] Cools J, DeAngelo DJ, Gotlib J, Stover EH, Legare RD, Cortes J, et al. A tyrosine kinase created by fusion of the PDGFRA and FIP1L1 genes as a therapeutic target of imatinib in idiopathic hypereosinophilic syndrome. New Engl J Med 2003;348:1201–14.

[9] Bach MK, Brashler JR, Stout BK, Johnson HG, Sanders ME, Lin AH. Activation of human eosinophils by platelet-derived growth factor. Int Arch Allergy Immunol 1992;97:121–9.

Yuko Ishii
Yoshikazu Ito*
Yuzuru Kuriyama
Tetsuzo Tauchi
Kazuma Ohyashiki
*First Department of Internal Medicine
Tokyo Medical University, 6-7-1 Nishi-Shinjuku
Shinjuku-ku, Tokyo 160-0023, Japan*
*Corresponding author. Tel.: +81-3-3342-6111x5895
fax: +81-3-5381-6651
E-mail address: yito@tokyo-med.ac.jp
(Y. Ito)

Identification of a SRC-Like Tyrosine Kinase Gene, FRK, Fused with ETV6 in a Patient with Acute Myelogenous Leukemia Carrying a t(6;12)(q21;p13) Translocation

Noriko Hosoya,[1] Ying Qiao,[1] Akira Hangaishi,[1] Lili Wang,[1] Yasuhito Nannya,[1] Masashi Sanada,[1] Mineo Kurokawa,[1] Shigeru Chiba,[1,2] Hisamaru Hirai,[1,2] and Seishi Ogawa[1,3]*

[1]Department of Hematology and Oncology, Graduate School of Medicine, University of Tokyo, Tokyo, Japan
[2]Department of Cell Therapy and Transplantation Medicine, University of Tokyo Hospital, University of Tokyo, Tokyo, Japan
[3]Department of Regeneration Medicine for Hematopoiesis, Graduate School of Medicine, University of Tokyo, Tokyo, Japan

The SRC family of kinases is rarely mutated in primary human tumors. We report the identification of a SRC-like tyrosine kinase gene, FRK (Fyn-related kinase), fused with ETV6 in a patient with acute myelogenous leukemia carrying t(6;12)(q21;p13). Both reciprocal fusion transcripts, ETV6/FRK and FRK/ETV6, were expressed. In ETV6/FRK, exon 4 of ETV6 was fused in-frame to exon 3 of FRK, producing a chimeric protein consisting of the entire oligomerization domain of ETV6 and the kinase domain of FRK. The ETV6/FRK protein was shown to be constitutively autophosphorylated on its tyrosine residues. ETV6/FRK phosphorylated histones H2B and H4 in vitro to a greater extent than did FRK, suggesting it had elevated kinase activity. ETV6/FRK could transform both Ba/F3 cells and NIH3T3 cells, which depended on its kinase activity. Moreover, ETV6/FRK inhibited ETV6-mediated transcriptional repression in a dominant-negative manner. This report provides the first evidence that a SRC-like kinase gene, FRK fused with ETV6, could directly contribute to leukemogenesis by producing an oncoprotein, ETV6/FRK, with dual functions: constitutive activation of the ETV6/FRK tyrosine kinase and dominant-negative modulation of ETV6-mediated transcriptional repression. © 2004 Wiley-Liss, Inc.

INTRODUCTION

The *SRC* gene was the first protooncogene isolated as the cellular homologue of v-*SRC*, the retroviral transforming oncogene of avian Rous sarcoma virus (Brown and Cooper, 1996). Since then, it has become clear that *SRC* is the prototype for a family of genes that encode nonreceptor tyrosine kinases implicated in a variety of cellular processes, including cell growth, differentiation, and carcinogenesis. The SRC family of kinases shares common structures consisting of an N-terminal unique domain, SRC homology 3 (SH3) and SRC homology 2 (SH2) domains, a kinase domain, and a short C-terminal regulatory tail (Brown and Cooper, 1996). They are normally maintained in an inactive state through phosphorylation of a critical C-terminal tyrosine residue (Tyr 530 in human SRC, Tyr 527 in chicken SRC) by the C-terminal SRC kinase (Csk) (Brown and Cooper, 1996). The SH3 and SH2 domains also participate in this negative regulation through intramolecular interactions (Brown and Cooper, 1996; Schindler et al., 1999; Xu et al., 1999; Young et al., 2001).

The SRC and its family member kinases have long been postulated to participate in oncogenic processes. Activated variants of SRC family kinases, including the viral oncoprotein v-SRC, are capable of inducing malignant transformation in a variety of cell types (Parker et al., 1984; Cartwright et al., 1987). Activation of SRC-like kinases recently was described in *BCR-ABL1*-expressing acute lymphoblastic leukemia in mice (Hu et al., 2004). Elevated expression and/or activity of SRC have been documented in several types of primary human tumors (Bolen et al., 1987; Ottenhoff-Kalff et al., 1992; Talamonti et al., 1993). However, for many years, structural abnormalities of the SRC family of kinases have been detected rarely in primary human tumors. Although Irby et al. (1999)